

Innovative High-Performance Deposition Technology for Low-Cost Manufacturing of OLED Lighting

Final Scientific/Technical Report
6/30/17

*DOE Agreement Number DE-EE0006263
NYSERDA Agreement Number 35375*

John Hamer – Principal Investigator
David Scott – Project Manager
OLEDWorks LLC

Prepared for:

US Department of Energy, EERE/BT and NETL

Brian Dotson – Project Manager

New York State Energy Research and Development Authority

Paul Vainauskas – Project Manager

Executive Summary

In this project, OLEDWorks developed and demonstrated the innovative high-performance deposition technology required to deliver dramatic reductions in the cost of manufacturing OLED lighting in production equipment. The current high manufacturing cost of OLED lighting is the most urgent barrier to its market acceptance. The new deposition technology delivers solutions to the two largest parts of the manufacturing cost problem – the expense per area of good product for organic materials and for the capital cost and depreciation of the equipment.

Organic materials cost is the largest expense item in the bill of materials and is predicted to remain so through 2020. The high-performance deposition technology developed in this project, also known as the next generation source (NGS), increases material usage efficiency from 25% found in current Gen2 deposition technology to 60%. This improvement alone results in a reduction of approximately \$25/m² of good product in organic materials costs, independent of production volumes.

Additionally, this innovative deposition technology reduces the total depreciation cost from the estimated value of approximately \$780/m² of good product for state-of-the-art G2 lines (at capacity, 5-year straight line depreciation) to \$170/m² of good product from the OLEDWorks production line.

Goals and Accomplishments

The objective of this project was to design and build a high-performance organic deposition source. During this project, four of these sources were installed in the OLEDWorks OLED production coater in a configuration such that the 4 nozzles can be used to simultaneously deposit a 4-component layer. These high-performance sources were installed in parallel to the existing prototype sources, converting the production deposition machine to a production machine with the following characteristics when operated in a semi-continuous mode:

1. Material usage efficiency – 40% overall, 60% with just the high-performance sources.
2. Takt time – 2 min average overall, 1 min with just the high-performance sources.
3. Throughput of good product (post yield and glass usage) – 7,800 m²/year using both high performance sources and prototype sources, 5,200 m²/year with just the high-performance sources.
4. Depreciation (just the coating machine – 5-year straight line) - \$100/m² overall for current semi-continuous production machine using existing prototype sources and new sources, \$14/m² for a Gen 4 continuous in-line production machine designed with the new sources.

The initial high-performance source, also known as the Next Generation Source (NGS), was successfully designed and constructed during this project. This prototype NGS has met the above goals and has paved the way for future improved high-performance sources.

The first objective of material usage efficiency has been achieved by the source. This metric is dependent on several external variables such as material, temperature, the quantity of frames and spacing between frames. An efficiency of approximately 57% was observed when depositing a host material but 47% when depositing a dopant material in the same run. The material utilization would be higher if the spacing between the frames were reduced and if there was less dead time when reversing the direction of the coater transport. In addition, the analysis is dependent on the estimated density of the materials. Overall, 57% is very close to the target and future tuning of the source and the production coater operation will increase the material usage efficiency even further.

The second objective was a takt time of 2 min overall or 1 min using only the high-performance sources. The NGS exceeds these goals when calculated using:

- 8 hr. shift – Total time available is 7 hr. or 420 min
- 2 min takt time – Need to make at least 210 panels
- 1 min takt time (NGS only) – Need to make at least 420 panels per shift
- **Cycle time** to make 450 panels using **original sources only** is 10 hrs.
 - 600 min /450 panels = 1.33 minutes/panel
- **Cycle Time** to make 450 panels using **both original sources and NGS (2 materials only)** is 8.5 hrs.
 - 510 min /450 panels = 1.13 minutes/panel

The 2 min takt time goal is exceeded with a cycle time of 1.13 minutes/panel using the original sources and NGS. The target takt time of 1 min using only the NGS will certainly be met due to the higher deposition rates (5 to 10X) over the original sources.

Processing throughput using a combination of original sources and the NGS loaded with 4 materials would increase significantly due to capability of coating two layers in a single pass. For example, a product requiring 15 coating passes could be reduced to 11 passes with the existing single NGS nozzle temperature limitation, a 27% reduction. Additional time savings would be realized since material burn-out normally done with original sources would be eliminated. Temperature adjustments required when changing materials in the original sources would also be eliminated. This time savings would be an additional ~10-15% reduction for a total of 37-42% time savings. If the NGS were equipped with individual nozzle temperature control allowing the use of materials with a wide range of evaporation temperatures or the product used similar temperature materials, the coating passes for the product could be reduced from 15 to 9, a 40%

reduction in time. Again, adding the time savings for eliminating burn-out and temperature adjustments, the total savings would be 50-55%. It has been demonstrated that an 8-frame, 15-layer run can be completed in 10 hours with traditional sources only. With a 37-42% reduction in time using the current configured combined sources, it would take 6-6.3 hours to complete coating those 8 frames. Hence it is not unreasonable that 30+ frames each loaded with 4 x gen 2 size glass ($0.6956\text{ m}^2/\text{frame}$) can be coated in a 24 hour. period. Operating on a 24/7 schedule for the full year without labor constraints, approximately 7600 m^2 can be coated with the combined original sources and NGS.

Processing throughput using the NGS only, compared to original sources, would also increase since coating speeds can be increased due to the large rate range capability. For our test 15-layer product coating 8 frames in 10 hours with original sources, approximately 19 frames can be processed per day, or approximately $\sim 4800\text{ m}^2$ of glass per year. The throughput with NGS would be similar when accounting for inserting pucks of material into the load lock assembly, bringing materials to rate, depositing on glass, waiting for rate decay to 0 A/s, and removing pucks from the load lock. For instance, the time required for inserting a puck in the NGS can be as long as the burn-out of material in original sources since the load lock must be evacuated to a pressure similar to the main chamber pressure. Again, the distinct advantage of the NGS is its high deposition rate capability which can allow faster track speeds. Simply increasing the track speed by 20% can increase throughput by the same amount. Based on rate data collected during experimentation, processing capacity of $5800\text{m}^2/\text{yr}$ is possible using NGS only.

Project Activity Summary

Task 0 – Project Management

This task included general project management support for meeting DOE reporting requirements, including regular conference calls, unscheduled calls, monthly, quarterly, and phase report generation, and participation in DOE workshops and conferences. All reporting requirements have been met. Several conflicts arose between shared resources and multiple projects resulting in delays. Three no-cost extensions were approved to allow completion of the project. Progress has been tracked using a regularly updated Gantt chart.

Budget Period 1 – Phase 1: Design, Fabrication, and Testing of Preliminary Vaporizer and Nozzle

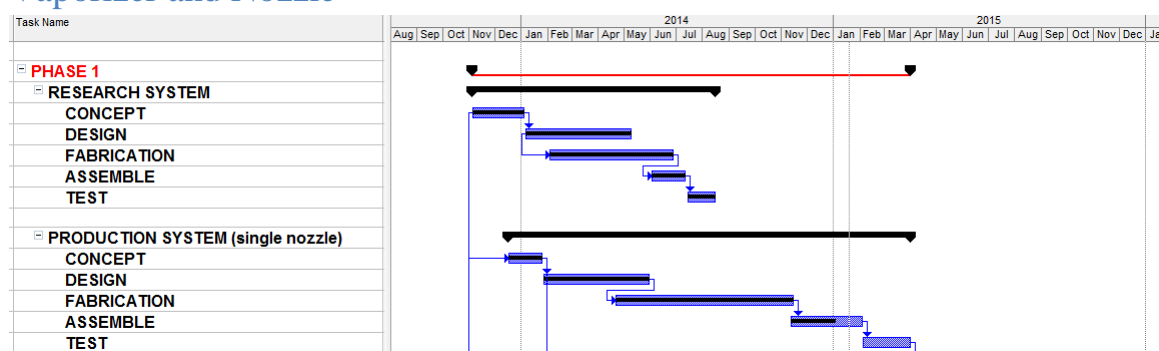


Figure 1. Gantt Chart Progress of Phase 1.

Task 1- Design Vaporizer Chambers

In this task, the external vaporizer chambers and mechanism were designed by OLEDWorks and manufactured by custom vacuum equipment fabricators. The design includes the following features:

1. Vaporizer located outside the vacuum chamber of the deposition coater.
2. Ability to load OLED organic material into vacuum in a removable crucible through a load lock.
3. Ability to rapidly heat and cool the material in the crucible.
4. Ability to direct the vapor into the conduction tube for transport to the OLED deposition machine.
5. Ability to interface with existing research OLED deposition machine.
6. Ability to control vaporizer with user interface and data collection capabilities.

The hardware mechanism was designed and simulated in Solidworks to ensure the above criteria were met. One of the most important design features is the ability to remove unused material relatively quickly and insert new. The removable material crucible eliminates the need for burning out unused material saving much time and material.

Simulations included thermal modeling to verify the design. The thermal modeling results indicated the vaporizer is free of cold spots and is capable of rapidly heating and cooling the material in the crucible. Figure 2 is a steady-state thermal model of a portion of the system verifying there are no cold spots.

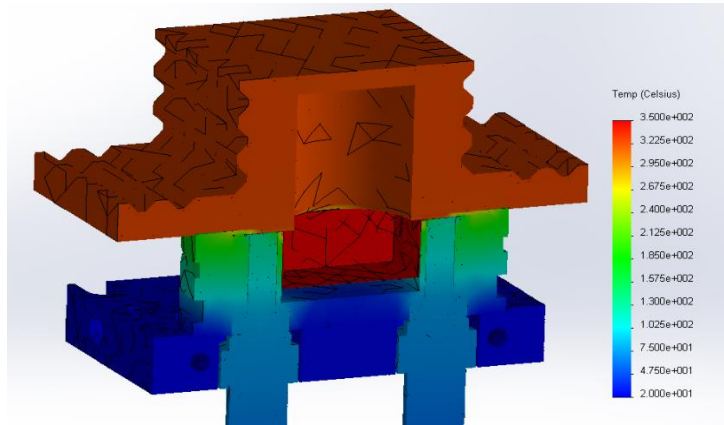


Figure 2. Steady-state thermal model of heated vaporizer system.

The cooling rates of the material crucible with and without the cooling plate were modeled after disabling the heating element. Both cases result in acceptable temperatures in under 5 minutes.

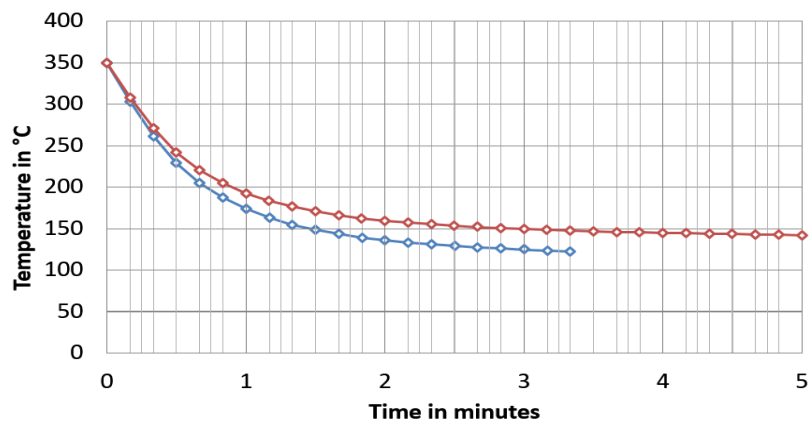


Figure 3. Cooling of material crucible with (blue) and w/o (red) active cooling.

Heating the material quickly was not a concern. A power supply capable of sourcing 200A was chosen to heat a relatively small thermal mass in a vacuum. The heater can be modeled as a 1Ω resistor producing 200W at 200A ($P = I * V$). 200W is more than enough to vaporize the organic materials in a short amount of time.

Task 2 – Build and Test Vaporizer Chamber

Initially, one vaporizer was built and tested by attaching it to an existing OLEDWorks R&D coater. Control hardware and software was developed utilizing a PLC and HMI operator interface. See Figure 4.

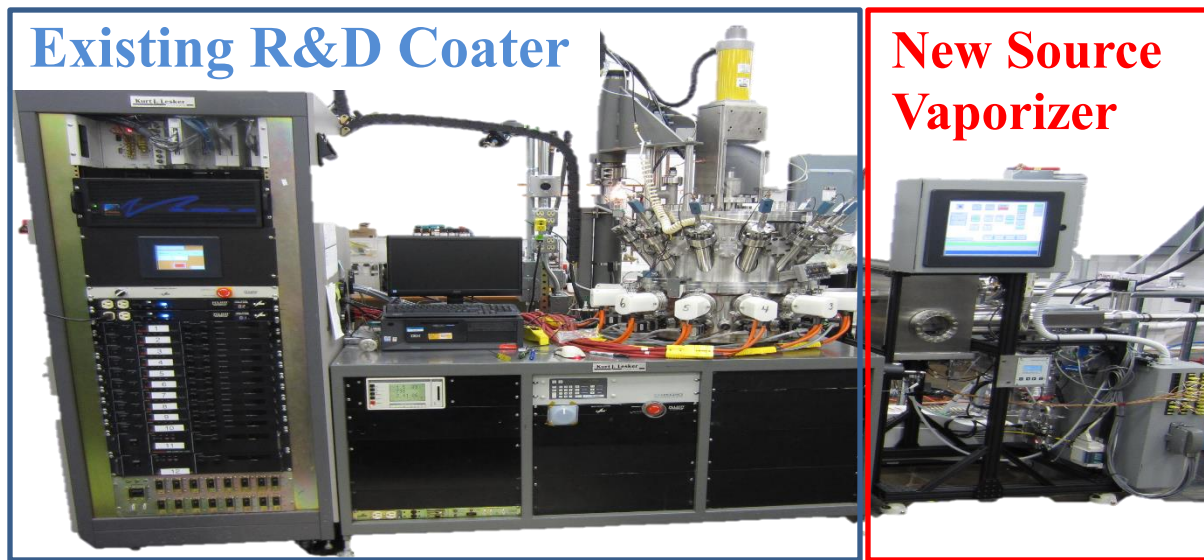


Figure 4. R&D Coater with New Source Attached.

The prototype source was tested by making OLED devices side by side with the original R&D coater's sources. The material was piped into the R&D chamber from the new source through a heated tube. Then the material is deposited through a single orifice from a temporary nozzle. Figure 5 displays the temporary nozzle alongside the original R&D sources with the orifice circled.

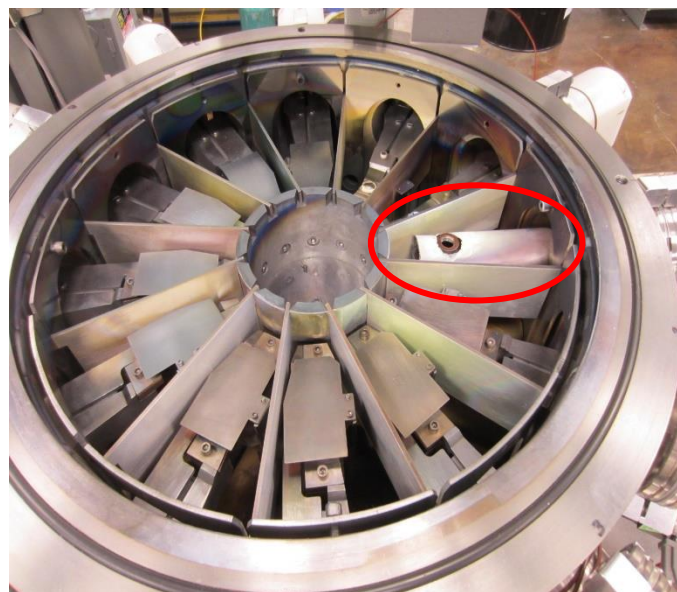


Figure 5. New Source Nozzle Inside R&D Coater.

The performance of the new vaporizer was determined, as well as the limits of its capabilities. The performance targets for the vaporizer include:

1. Ability to heat material in crucible to operating temperature within 5 minutes
2. Ability to cool material in the crucible to safe removal temperature within 10 minutes
3. Ability to generate vapor over a wide dynamic range – from 0.01 g/hour to 10 g/hour.
4. Ability to make good OLED devices (compared to standard evaporation crucibles) in side-by-side fabrication – testing one material at a time.
5. Ability to handle heat sensitive compounds – under operating conditions for 30 min.

First, the ability to generate vapor and the dynamic range was demonstrated. The volume in g/hour was calculated by observing the deposition rate of material in Å/s using QCMs. The dynamic range of vapor generation exceeds the design criteria (0.0042 – 10 g/hour – 2,400:1).

The vaporizer is capable of heating materials to operational temperatures in approximately 5 minutes. A multistep and gradual warmup process is used to prevent component damage due to thermal stress. Initially, the material crucible is preheated to a temperature below the material's vaporization point. The preheating reduces both thermal stress and the time required to reach operating temperature. During warmup, the power is continually stepped upward until rate is observed. Finally, closed loop (PID) control is enabled which precisely and quickly controls the deposition rate. Figure 6 is a snapshot of the material heating, deposition, and cooldown process.

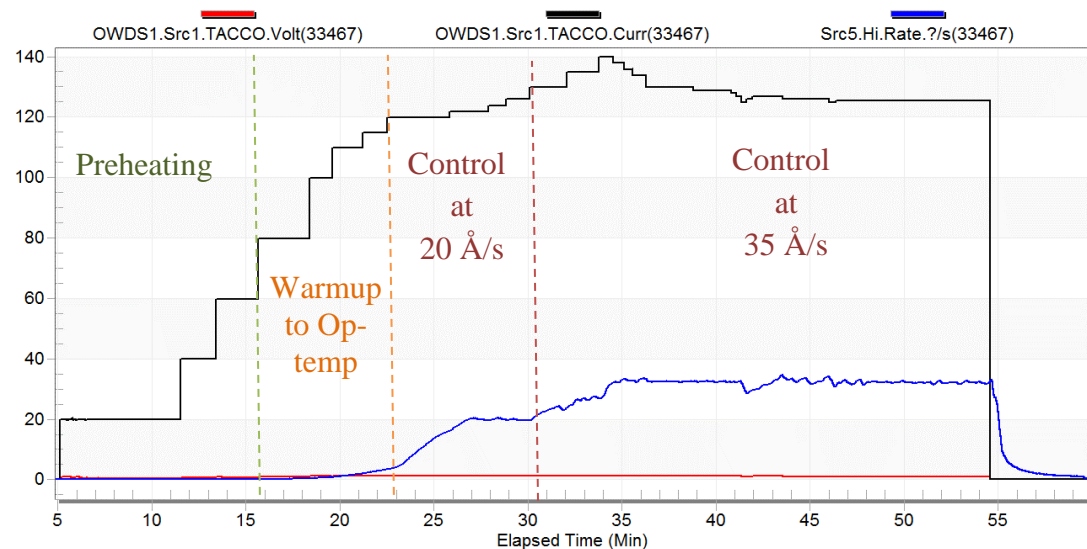


Figure 6. Plot of current(A) and deposition Rate.

After disabling power to the material crucible, the deposition rate drops quickly to negligible levels well within 10 minutes. See Figure 7. Afterwards the material can be removed and reused instead of burned off and wasted. This is significant improvement over the existing prototype sources in terms of saving time and materials.

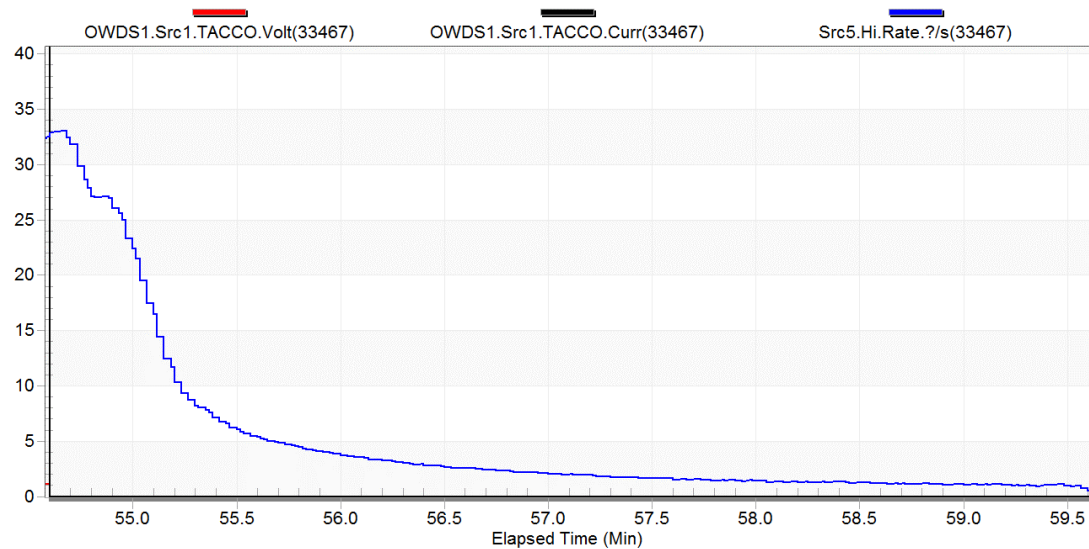


Figure 7. Cooldown curve. Rate < 0.5 Å/s in 5 minutes.

Furthermore, OLED device performance characteristics such as color spectra, voltage, efficiency, and lifetime were scrutinized when using the new source. OLED devices were produced in the research coater with a variety of host and dopant materials deposited by the new source. In general efficiency, color spectra, voltage, and lifetime were equal or improved when compared to the controls. Most notably, improvements over the controls were observed when depositing thermally sensitive compounds (dopants) using the new source. These results are displayed below in Figures 8 through 11 respectively.

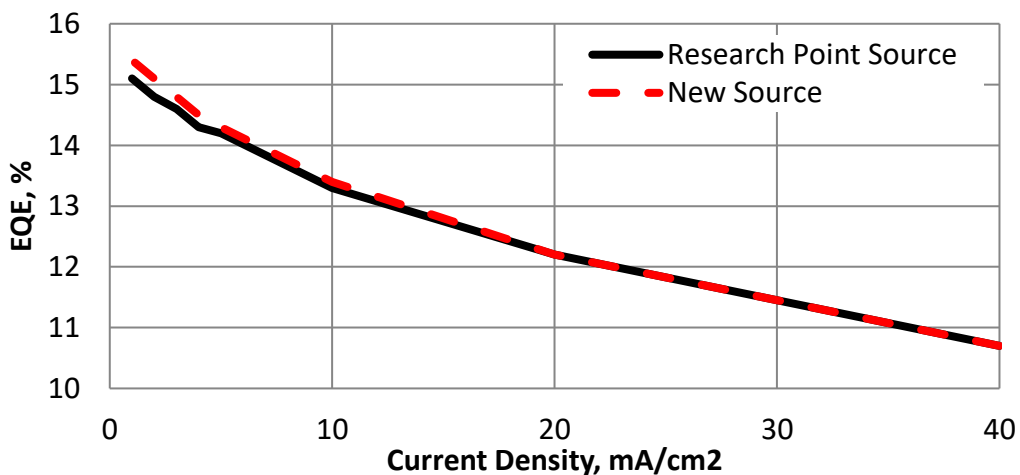


Figure 8. Yellow Phosphorescent Dopant #2 – Efficiency

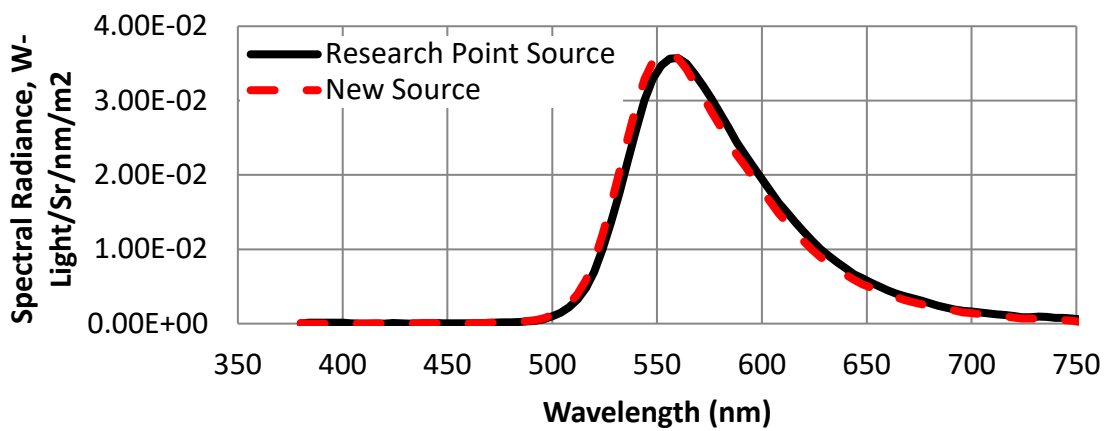


Figure 9. Yellow Phosphorescent Dopant #2 –Spectral Radiance

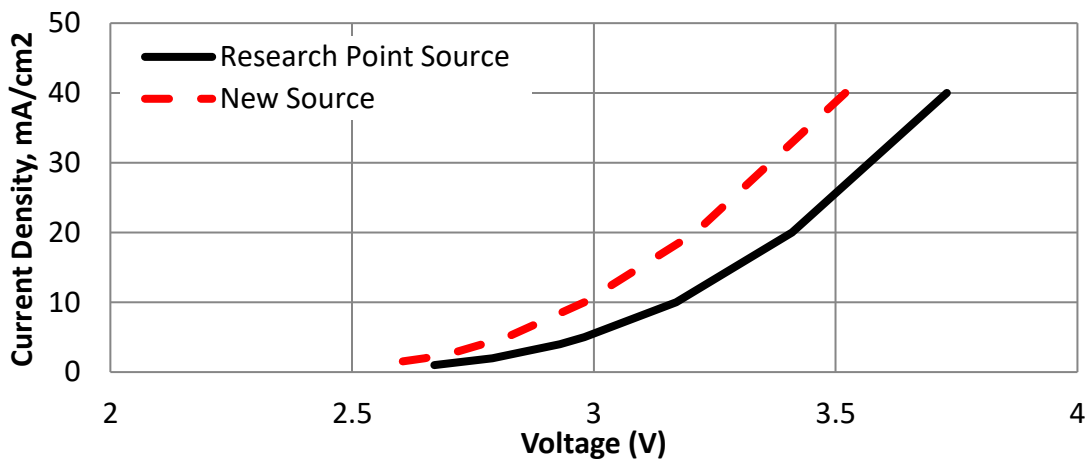


Figure 10. Yellow Phosphorescent Dopant #2 –Voltage

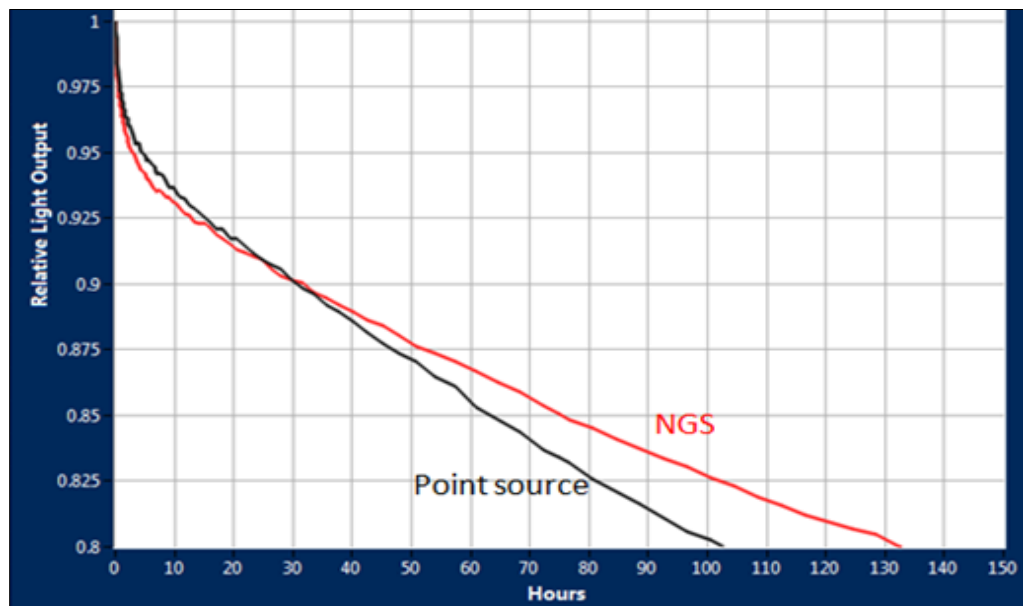


Figure 11. Lifetime comparison with dopant deposited by new source.

Task 3 – Design, Build, and Test Nozzle and Conduction Tube

One nozzle and conduction tube were designed, built, and tested in the production coater in conjunction with the new vaporizer from tasks 1-3. The production coater was modified to accept the new nozzle and vaporizer. The controls for the new equipment are integrated with the existing system software of the production machine including sensors, controls, interlocks, warnings, alarms, emergency conditions, data collection, and operator interface. The new source was tested by making OLED devices side by side with the existing prototype sources. The performance and limitations of the new source with the new conduction tube and nozzle were determined for single material layers. The performance targets for the vaporizer and nozzle are:

1. Task 2's criteria.
2. Ability to uniformly deposit the OLED organic material uniformly within +/-10% across the 730mm wide coating width.
3. Ability to regulate the vapor flux using a valve and feedback control from a rate sensor to within +/- 5% of the target rate.
4. No significant build-up of residual OLED materials or residue on or inside any parts of the equipment that would require frequent maintenance.
5. Material usage efficiency of 60%.
6. Ability to deposit materials for typical layers at a takt time of 60 sec.

Design and Simulations of Nozzle

The nozzle was designed with four large chambers for deposition uniformity, thick walls for isothermal operation, and channels to hold swaged heaters. The nozzle plume was simulated for a variety of hole patterns to determine the optimal hole pattern. The resulting plume, as shown in Figure 12, verified a material usage efficiency of 60% would be met with a 730mm wide coating window.

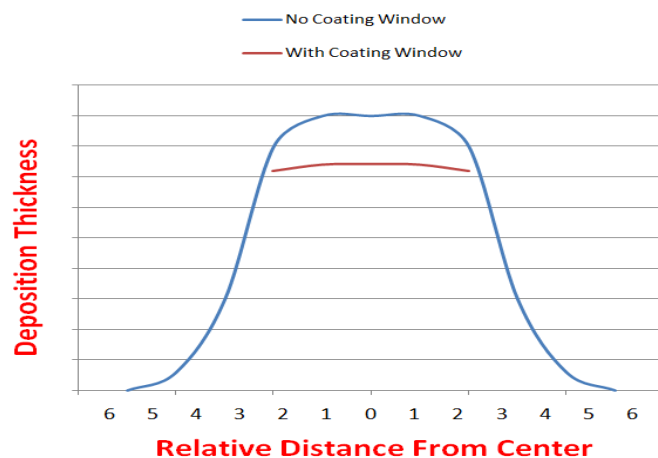


Figure 12. Nozzle plume simulation.

Heater channels were milled into the nozzle and spaced to heat uniformly. Ultra-high vacuum heaters were swaged into these channels. See Figure 13. The nozzle design was verified using thermal analysis.

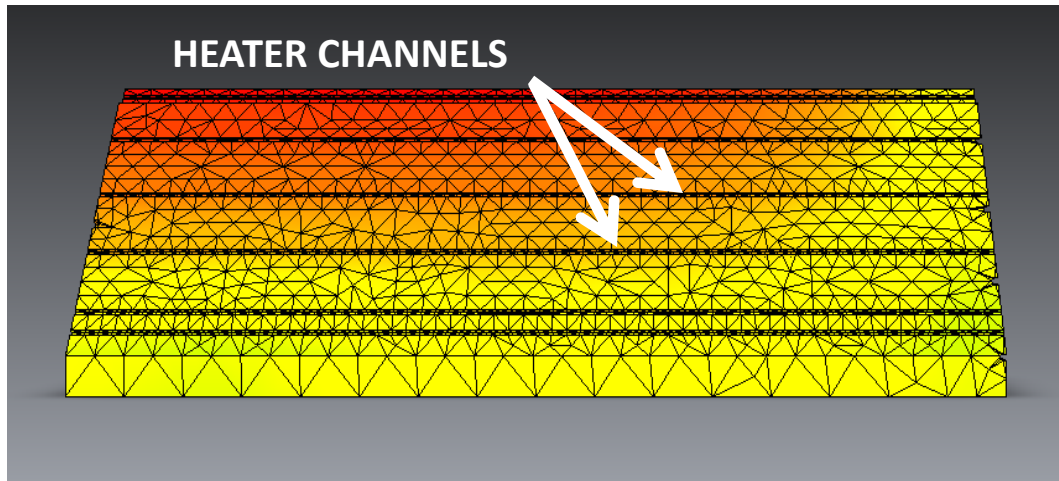


Figure 13. Nozzle thermal simulation.

Testing of the Single Vaporizer Source in Production Coater.

The source was installed in the OLEDWorks production coater adjacent to the original vapor deposition sources as shown in Figure 14. An initial control was established by leaving the new source cool and making OLEDs using the original sources. Several cycles of testing and improvements followed. Calibrations were run to determine deposition uniformity and the tooling factors of the QCM rate monitors.

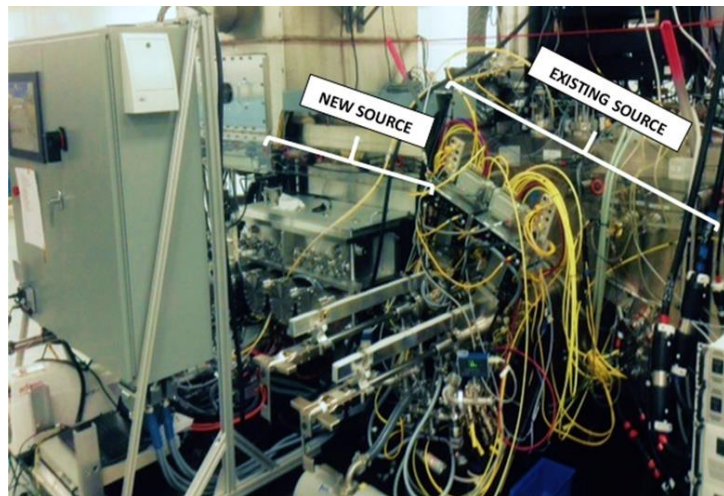


Figure 14. New Source Adjacent to Existing Source.

Thermal and Power Dynamics of the System.

During the first warm-up of the new nozzle in vacuum, all heaters were driven to approximately 280°C using 15% power. A fixed power was chosen to allow observation of the nozzle's thermal energy characteristics. The resulting nozzle temperatures were

considerably uniform ($\pm 10^\circ\text{C}$) as shown in Figure 15. Cooler temperatures were observed in the bottom center due to a lack of heat shielding, heating elements, and only one conduction tube attached. This was expected with only one source attached.

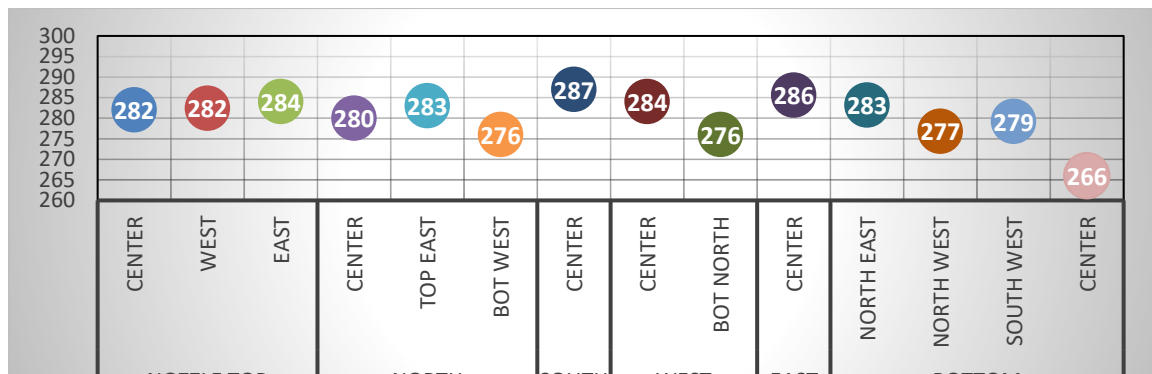


Figure 15. Nozzle Temperatures After 3 Days with all Heaters Operating at 15% Power.

After enabling and tuning the closed loop temperature controls, all heater zones maintain temperature within $\pm 1^\circ\text{C}$. Table 1 shows the stability of the system at 350°C as well as the power and temperature distribution. As expected, zones with comparable mass, surface area and shielding have similar power requirements. Overall, the system uses relatively low amounts of power to maintain high temperatures.

System	Temp. SP (°C)	Temp. Meas. (°C)	Output (%)	Resistance (Ω)	Power Watts
Injector Body	325	325	1.3%	4.3	44
Injector Valve	350	349	10.1%	14.6	100
Injector Band - Small	350	350	4.6%	60.7	11
Conductance Tube Center	350	350	8.5%	21.6	57
Injector Band - North (1/2)	350	350	8.6%	31.9	39
Cond Tube Band Port Top	350	351	13.8%	61.4	32
Cond Tube Band Port Bottom	350	350	9.0%	61.5	21
Nozzle Bottom - NW	350	350	38.8%	66.7	84
Nozzle Bottom - SW	350	350	48.6%	67.3	104
Nozzle Bottom - NE	350	350	54.7%	66.4	119
Nozzle Bottom - SE	350	350	37.5%	66.7	81
Nozzle Side Plate - N (center)	350	350	23.7%	23.2	147
Nozzle Side Plate - S (center)	350	350	17.3%	22.8	109
Nozzle End Plate - W (center)	350	350	13.5%	103.7	19
Nozzle End Plate - E (center)	350	351	0.0%	103.4	0
Nozzle Top (center)	350	350	20.8%	27.5	109
Total System Power (Watts)					1074
Total Nozzle Power (Watts)					771

Table 1. System Heating and Temperature Dynamics.

Initial Testing

Manual power control of the vaporizer crucible was used to control the rate of deposition during the first calibration. Two frames of glass substrates were run, one at a high rate and one at a low rate. The rates are displayed in the operator interface as depicted in Figure 16. Two curves are shown. One is a high rate sensor (less sensitive), Src1 Hi, and one is a low rate sensor (more sensitive), Src1 Lo.

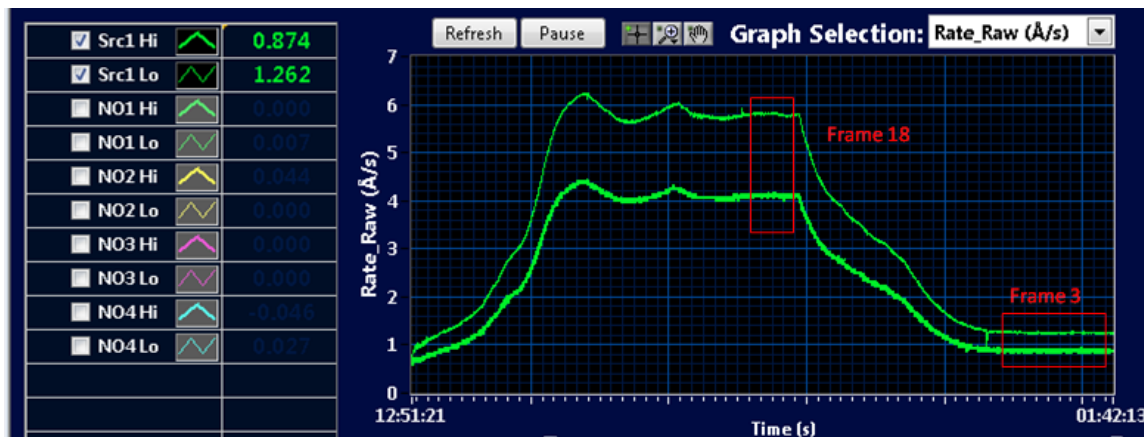


Figure 16. Rate Observed Using Manual Power Control.

An estimate of total deposited thickness was calculated using the above rates and compared to the measured thickness. The actual thickness deposited on the glass substrate was measured using ellipsometry. The ellipsometry results, shown in Figure 17, indicate exceptionally uniform material deposition on the calibration frames. Most importantly, uniformity was maintained at both high and low rates.

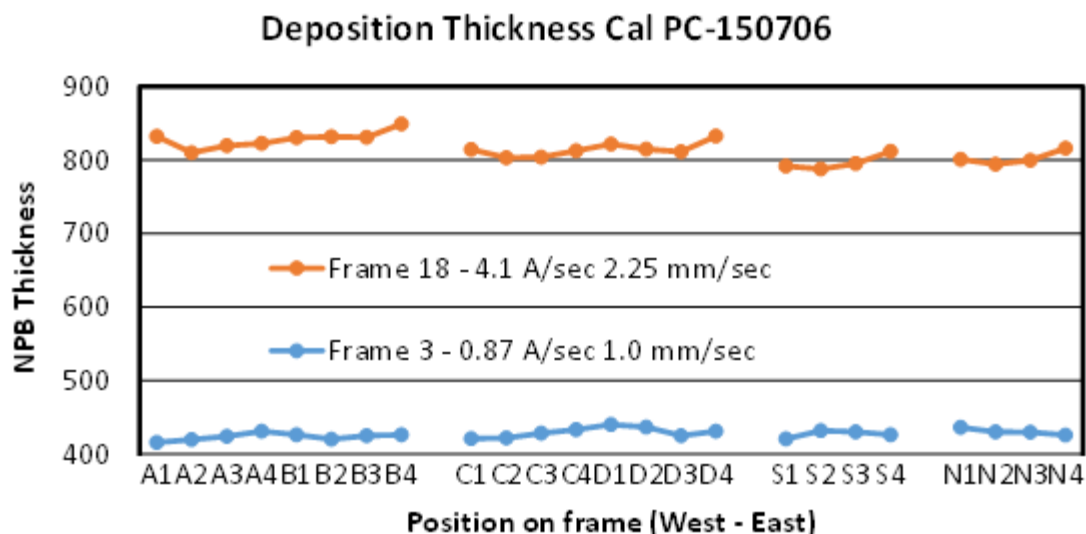


Figure 17. Calibration Material Uniformity.

The ratios of measured and predicted thicknesses yields each sensor's respective tooling factor. A consistent tooling factor is important for device repeatability. Table 1 lists predicted thickness, measured thicknesses, and calculated tooling factors.

Predicted Deposition Thickness			Calculated Tooling Factors	
Hi Rate QCM (Å)	Low Rate QCM (Å)	Actual Thickness (Å)	Hi Rate QCM	Low Rate QCM
148.7	215.1	427.3	2.9	2.0
310.1	438.7	814.0	2.6	1.9

Table 2. Calculation of Tooling Factors

After installing the source, reaching baseline pressure (10^{-7} torr) took significantly longer than normal. The increased chamber volume and surface area is largely responsible. However, devices manufactured using the existing deposition sources had reduced lifetimes with the new source installed, as shown in Figure 18. Device lifetimes returned to normal after the removal of the new source and chamber cleaning. Evidently, there were materials outgassing from the source, slowing pump down, and contaminating the standard process.

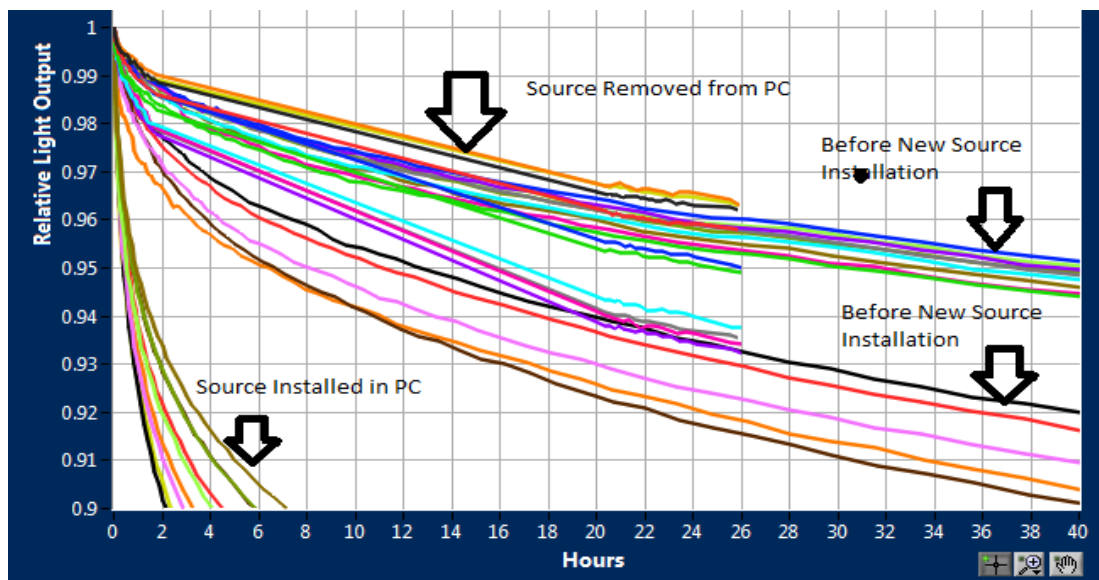


Figure 18. Device Lifetime Comparison.

Possible causes of contamination were investigated. Using a small research coater, OLED lifetime experiments were performed with samples of suspect contaminating components. The heater wires were tested due to a suspicious coating found on the fiberglass insulation. Additionally, visible contamination was found on the sides of the nozzle. Screws removed from the nozzle were also tested. Degradation of OLED device lifetimes due to tested contaminates are shown in Figure 19. Evidently, the wire insulation decreased overall device lifetime while the substance(s) on the nozzle caused a rapid initial degradation in device lifetime.

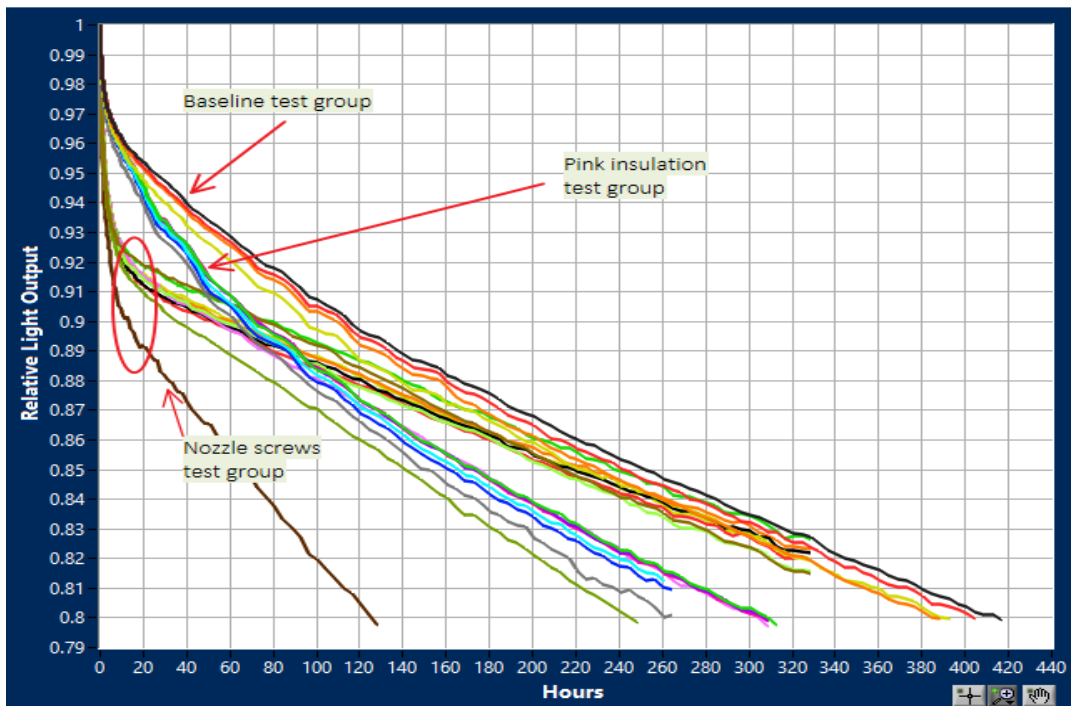


Figure 19. AC1 Device Lifetimes with and without Contaminates.

The following actions were taken to remove all sources of contamination.

- Nozzle heaters with fiberglass insulated leads were removed.
- New nozzle heaters with Teflon insulated wire leads were installed.
- Steel screws were removed to prevent virtual leaks.
- The nozzle chemically passivated by a third party
- All parts were thoroughly cleaned with strong solvents.

OLED lifetimes will be revisited after contamination cleanup in the next section. The lifetimes of OLED devices made with the new source will also be observed.

First Run Making OLEDs

The next generation source was re-calibrated using three frames at three different rates prior to the making OLEDs in the production coater. Each frame contained glass chips spread widthwise. The run results are shown in Table 3. Tooling factors for the high and low QCMs were calculated. The tooling factors are relatively consistent but are clearly a function of rate. The software was modified to automatically pick the best tooling factor using interpolation of the rate specified.

Frame	Rate (\AA/s) (tf=1)			Thickness (\AA) (tf=1)			Tooling Factor (tf)	
	Set Pt.	High QCM Average	Low QCM Average	High QCM Estimated	Low QCM Estimated	Measured	High QCM	Low QCM
1	1	1.03	1.94	58.4	109.9	195.2	3.35	1.78
2	2	2.14	4.02	121.3	227.8	356.3	2.94	1.56
3	3	3.11	5.9	176.2	334.3	515.9	2.93	1.54

Table 3. Calibration Data. Initial Tooling Factor set to 1. (Assumes QCM and Substrate Deposition Rates are 1:1)

Deposition uniformity across the frame was excellent, $\pm 2\%$, as indicated by Figure 20. Results from this calibration are consistent with the prior calibrations. These results exceed the goal of $\pm 10\%$.

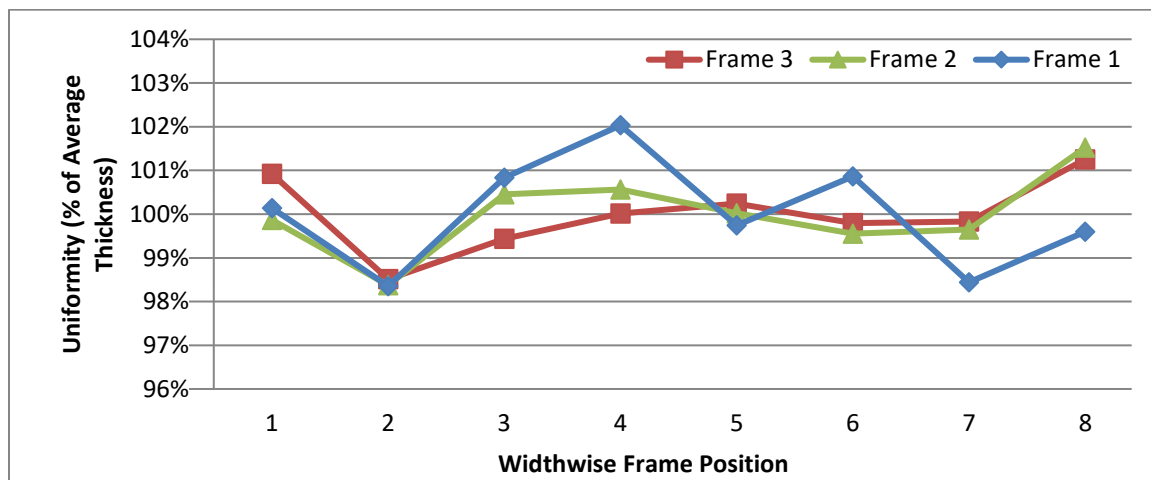


Figure 20. Plot of Calibration Uniformity.

Next, closed loop PID rate control was implemented. The controller can vary the deposition rate quickly, rejecting any disturbances such as temperature variations and gradual material depletion. Figure 21 displays the closed loop response of the system for a fixed power and varying rate set points. Step changes in rate set point ranged from 0 to 6 \AA/s . The QCM tooling factors from Table 3 have been applied so the rates represent the actual amount of material depositing on passing devices in \AA/s . The rate settling time due to a step change in set point is approximately 20s.

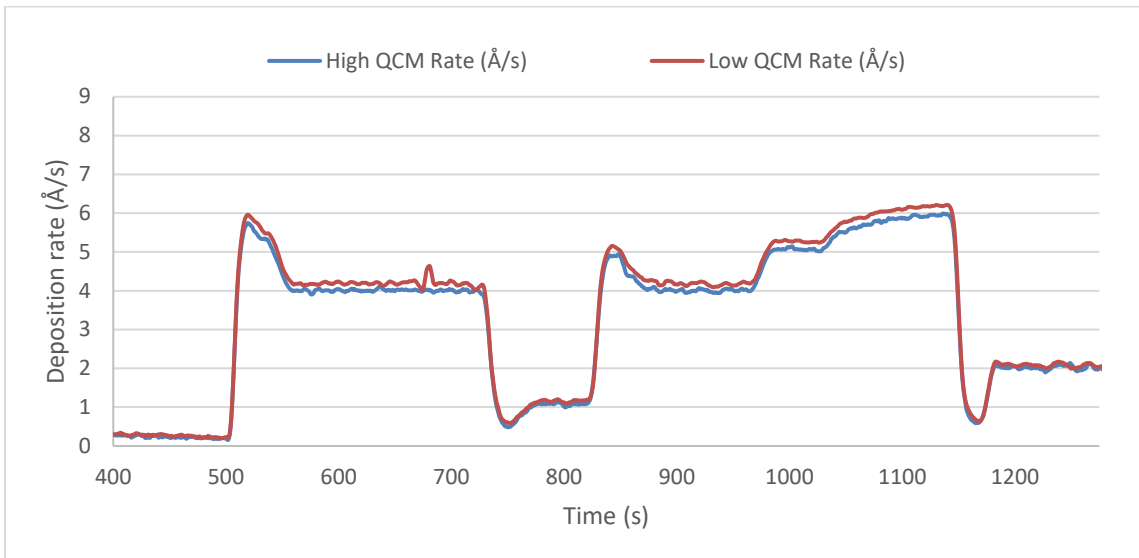


Figure 21. Closed loop control of rate.

Finally, the first experimental run making OLEDs was completed using the next generation source. Two frames of devices were coated during this run. Frame A devices served as controls and were deposited entirely using the original sources. Frame B contained devices where the electron transport layers were deposited by the next gen source.

The resulting OLED lifetimes of Frame B are very similar to Frame A controls. These lifetimes are also comparable to quality control runs prior to the installation of the next generation source. Figure 22 represents the lifetimes of several OLED devices made with the NGS alongside several controls. Evidently, there is no further contamination in the deposition process.

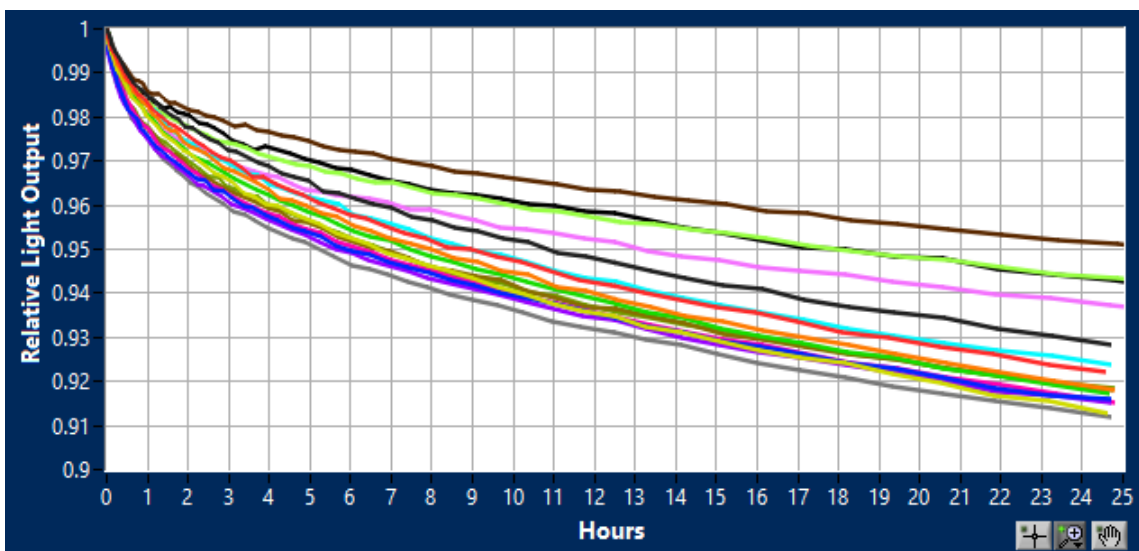


Figure 22. Lifetime comparison of devices made with next generation source.

Not only did the OLED devices have comparable lifetimes, the OLEDs exhibited similar electrical and spectral characteristics as shown by Figures 23 - 25.

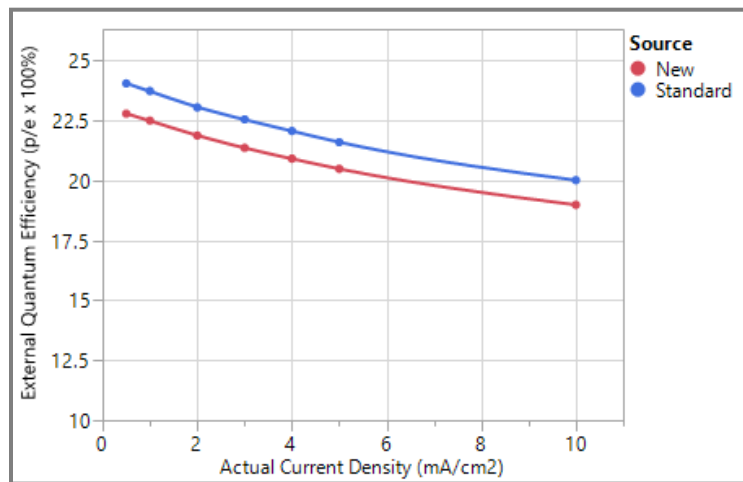


Figure 23. Efficiency vs Current Density.

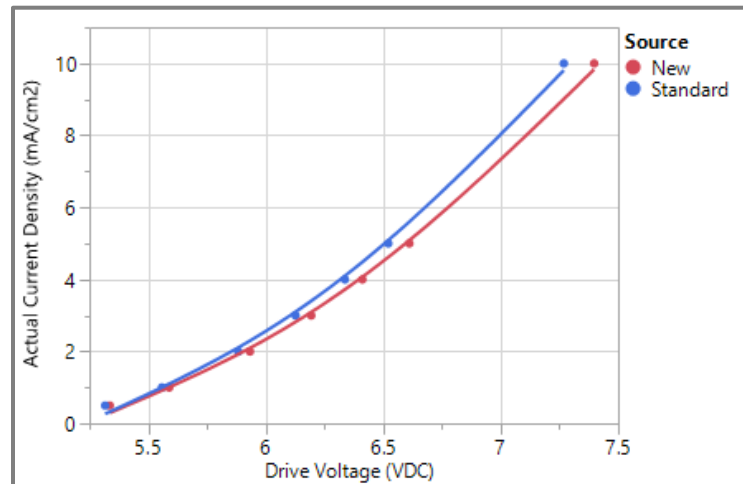


Figure 24. Current Density vs Drive Voltage.

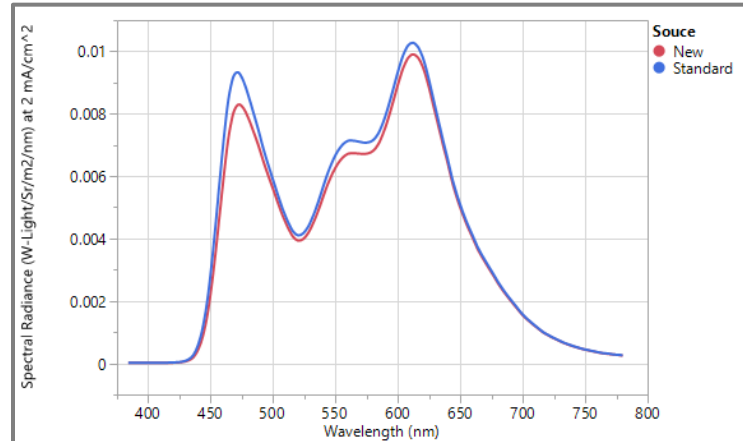


Figure 25. Spectral Plot.

Thermal Testing

The temperatures of glass substrates were measured while in proximity to the nozzle. The amount of radiant heat was a concern because temperatures above 100°C can degrade OLED devices. Tests were performed using temperature stickers to estimate the maximum temperatures OLEDs could be exposed to during the deposition process. The temperature stickers were attached to a frame and then passed over the nozzle while heated to temperatures up to 350°C. The stickers indicated temperatures higher than 125°C. To reduce the amount of heat reaching the substrate, the top nozzle shield was electro polished lowering the material emissivity. Also, a thin insulator was installed between the nozzle and the top shield. Follow-up testing determined the substrates were still exposed to temperatures greater than 125°C.

Accurately measuring the temperature of thin films is difficult on moving glass substrates in a high vacuum due to their transparent nature. Therefore, a new method was developed using NPB (an OLED organic hole transporting material) as a temperature indicator. NPB's glass transition temperature (Tg) is approximately 95°C, one of the lowest for organic materials. If the film is heated to temperatures above the Tg of 95°C, the material begins to crystallize and appear hazy.

Utilizing the glass transition temperature of NPB, the approximate temperatures of the deposited films could be observed. With the nozzle at a temperature of 350°C, three groups of calibration samples were deposited using NPB each at a different deposition rate. The lower deposition rates required multiple consecutive passes to reach the target thickness. Consequently, these calibration chips were exposed to greater levels of IR heat. As shown in Figure 26, the samples exhibited an increasing amount of crystallization as a function of exposure time to the nozzle. OLED devices in a standard production run are only exposed to the nozzle once per layer. Consequently, additional temperature testing under normal operating conditions was necessary.

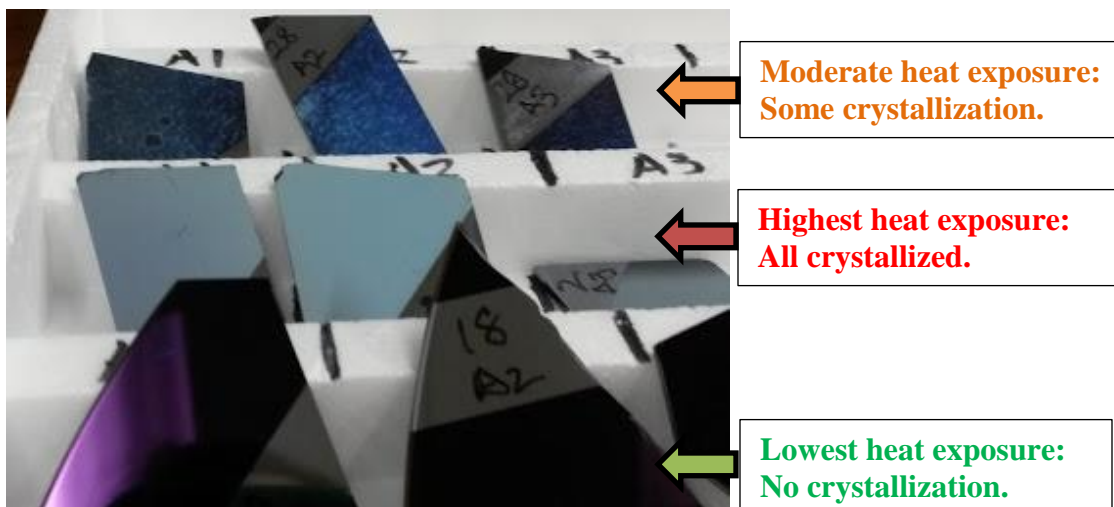


Figure 26. Crystallization of NPB Calibration Samples.

Thermal Effects on OLED Performance

A triple stack white run (PC1-160408) was performed using the source to deposit NPB. Frame A contained OLED devices deposited only with the original sources. Frame B devices utilized the source to deposit NPB layers. The results of the two frames and a previous run (PC1-160215) of the same formulation were compared. Figures 27 and 28 compare the resulting device color's and efficiency's respectively. Frame B devices have consistent color with some deviation to Frame A. However, when compared to the previous run, all device colors were significantly off. Efficiency was about 10% lower for Frame B devices. Similar behavior was exhibited by unrelated amber devices when passed over the 350°C source. Follow-up runs with the source cooled exhibited the correct color characteristics. This evidence suggests the nozzle at 350°C is overheating the devices and altering their color characteristics during normal operations conditions.

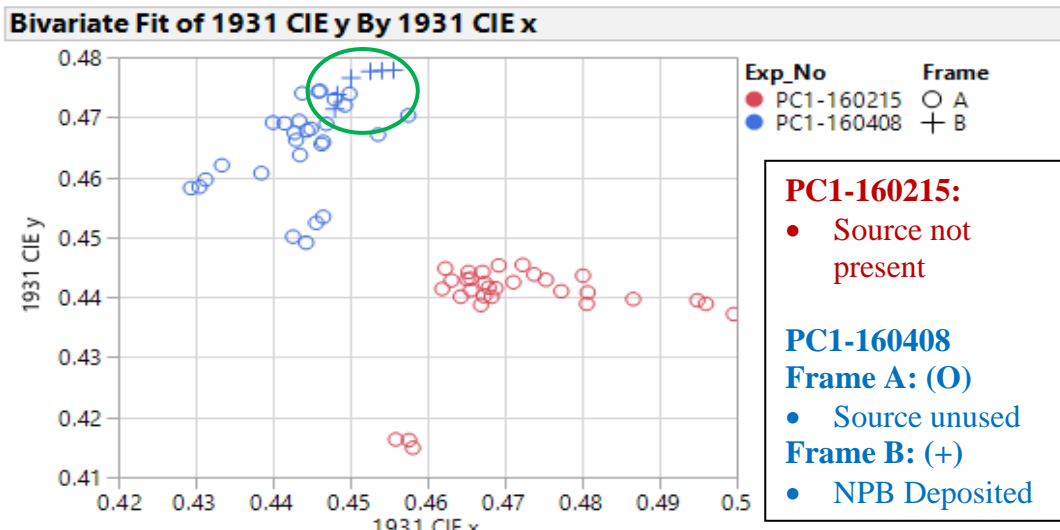


Figure 27. Triple Stack White Run Color Comparison.

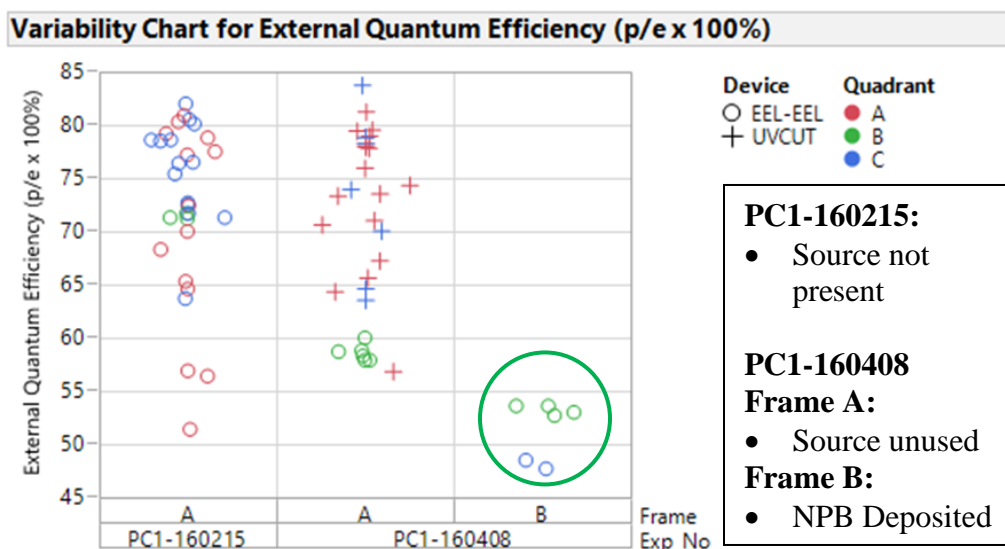


Figure 28. Triple Stack White Run Efficiency Comparison.

Budget Period 2 - Phase 2: Design Improvement, Fabrication of 4, and Testing in Production Chamber

Task 4 – Analyze Nozzle and Vaporizer Test Results and Modify Design

Using results of the testing on the first vaporizer and nozzle, some design improvements were made. The design was modified to accommodate 4 independent vaporizers and 4 independent nozzles to be integrated into one compact design. The design will resolve the temperature degradation of passing OLED devices and include the following features:

1. Ability to integrate 4 vaporizer units into closely packed space. Desired overall length is less than 1 meter.
2. Ability to integrate 4 nozzle units into closely packed space to enable co-deposition of 4 materials using overlapping plumes from a nozzle-to-substrate distance of 150-200 mm.
3. Ability to co-deposit 4 materials on the substrate in a small coating window. Desired length of coating window is less than 0.5 meters.
4. Ability of the temperature controls to independently simultaneously heat and cool the vaporizers.
5. Ability for reducing radiant energy to the substrate such that the temperature rise of the substrate over the 4 nozzles is less than 5°C at a takt time of 60 sec.

The system was designed to meet the above criteria during Task 3. The focus during Task 4 is primarily to debug and re-design before cloning the vaporizer three times.

Temperature Characterization Experiments

Evidently, OLEDs with temperature sensitive materials degrade due to radiant heat from the nozzle. Further testing was performed to characterize the effect of IR heat on passing OLED devices. The need for improved shielding was determined. With the nozzle at 350°C. The top shield reaches a warm 260°C. Estimations suggest passing substrates reach upwards of 150°C depending on the transport speed and the frequency of passes. This is consistent with prior temperature sticker results and crystallizing NPB samples.

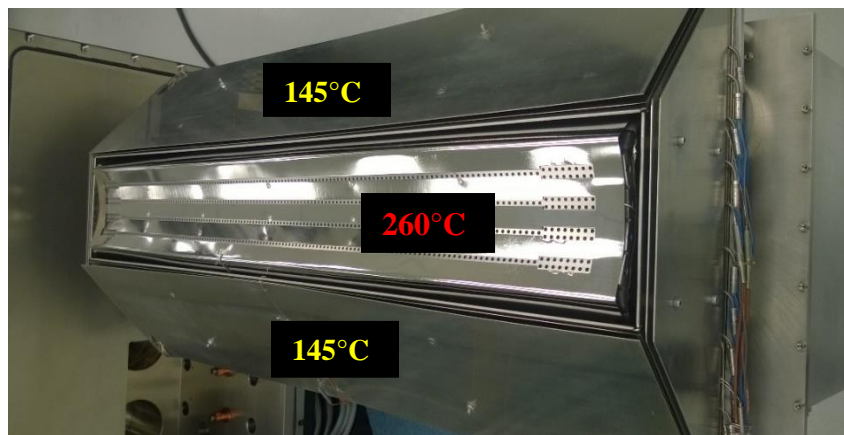


Figure 29. Temperatures of Nozzle Shielding w/ Nozzle at 350°C in vacuum.

Several iterations of experiments with increasing layers of temporary shielding revealed the limitations of passive cooling. Approximately 30 thermocouples were strategically placed to observe unknown temperatures. Points of interest included permanent shields, temporary shields, chamber, frame, and substrates. Figure 30 exemplifies the placement of shields and TCs for one iteration of experiments, featuring the greatest amount of temporary shielding. Foil was used as temporary shielding as shown in the right half of Figure 30.

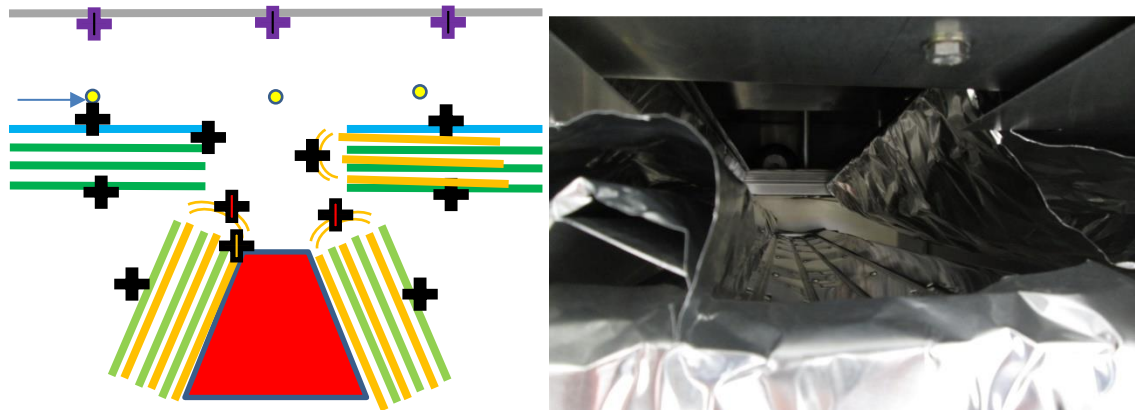


Figure 30. Shielding and thermocouple placement for thermal experiments.

The temperature rise curves for the glass substrates while in the coating window are summarized in Figure 31. As expected, additional layers of heat shielding decreased the heat load on the glass substrates. For reference, the heat load was also measured from the Original sources. The bottom two curves represent the Original heat load. The yellow curve (TC36 – Mask, Glass, Magnet E NGS Fri) represents the configuration in Figure 30 and the lowest heat load achieved with only passive shielding on the next gen source. Evidently, the best case next gen source with passive cooling is still not comparable to the original sources. Active cooling is needed to reliably reduce the heat load on OLED substrates.

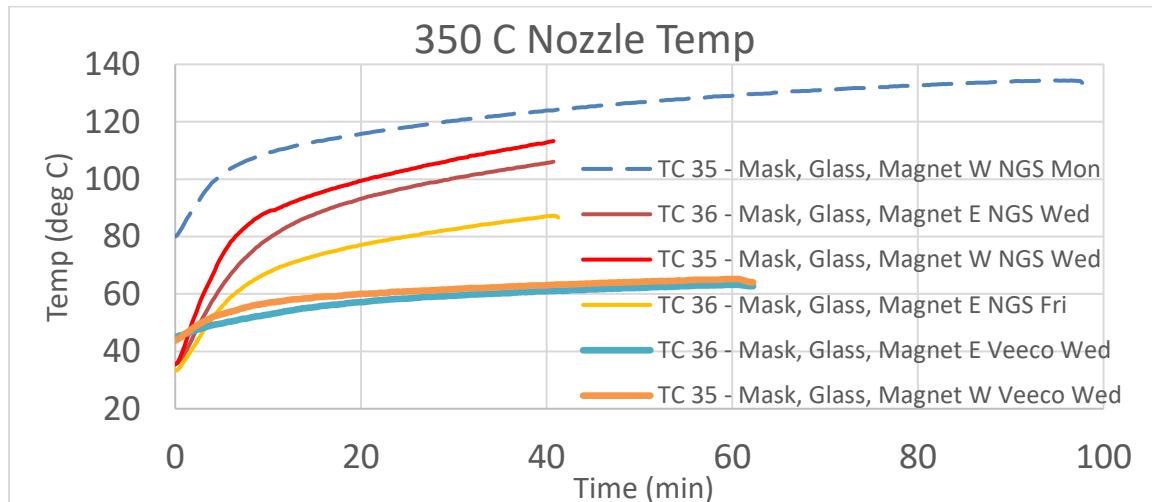


Figure 31. Temperature rise curves of substrates due to varying heat loads.

Design Improvement – Addition of Actively Cooled Shield

A variety of locations were considered and modeled in the design of actively cooled heat shielding. Two cooling plates as shown in Figure 33, were chosen as the best solution to reduce the heat load on OLED substrates. The design consists of two 1/8th inch copper plates with copper tubing. The plates are supported at the top of the nozzle and by aluminum shields mounted to the main nozzle support arms.

The actively cooled shielding was estimated to reduce the heat load on the OLED substrates by 30% and predicted to absorb 237W/m of energy from the chamber. This design will maintain OLED substrate temperatures well below a limit of 90°C.

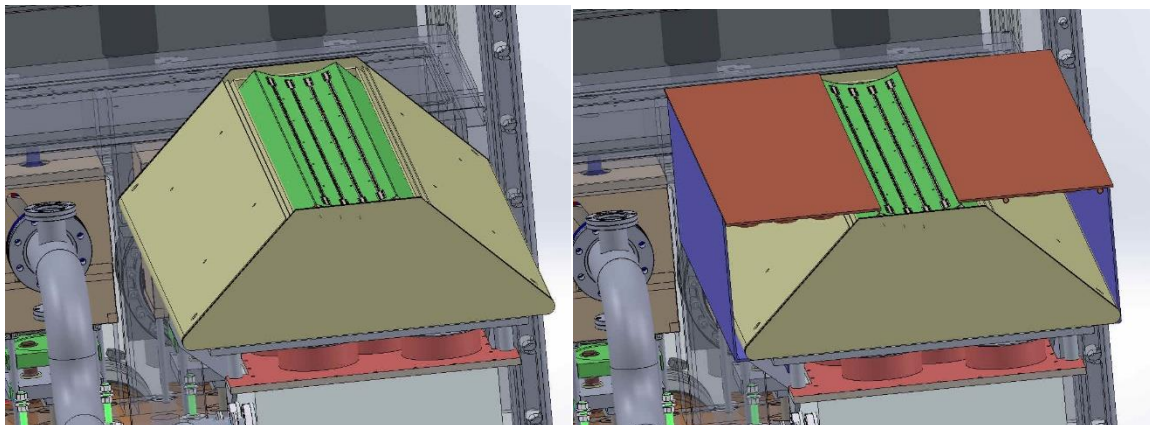


Figure 32. Source nozzle with and without active cooling.

After the edition of the active cooling shield as shown in Figure 33, ambient and OLED substrate temperatures were reduced to acceptable levels. The cooling shield design was very successful. With the nozzle heated to 300°C, the shield's surface reached a peak temperature of 22°C as measured by 4 fixed thermocouples.

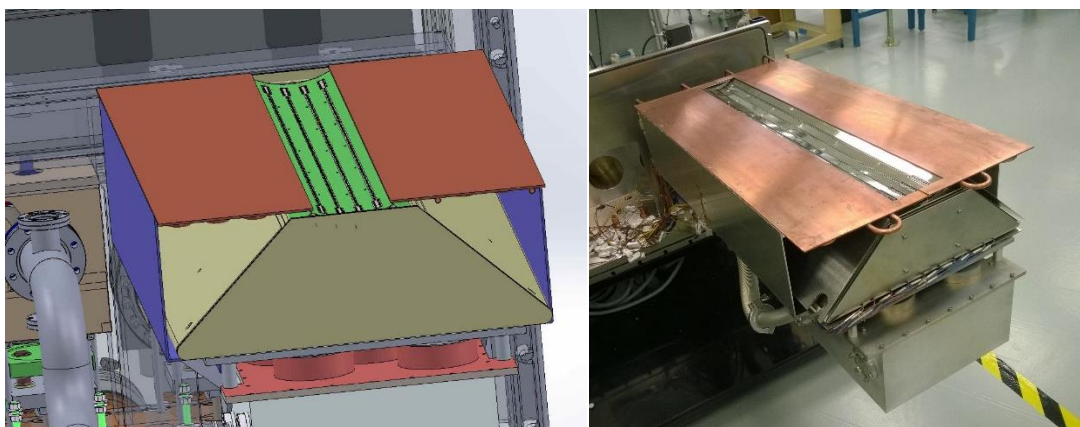


Figure 33. Source nozzle with new actively cooled shields.

Most importantly, OLED substrate temperatures remained well below the 90°C limit under high heat operating conditions (Nozzle Temperature =300C°). To measure the substrate temperatures, our custom designed temperature monitor (HOBO), as shown in Figure 34, was installed on a frame and exposed to actual deposition conditions during runs. The temperatures of four different locations on a frame were measured using the four thermocouple inputs.

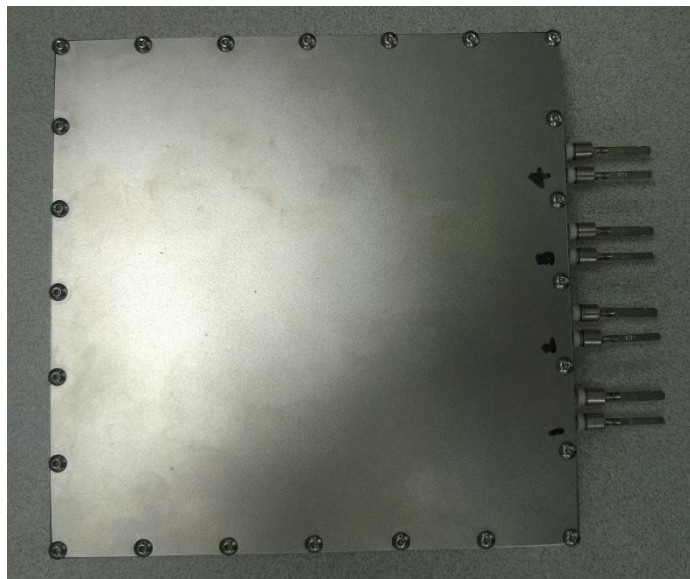


Figure 34. Vacuum Safe Temperature Monitor (HOBO).

Analyzing the temperature data from the HOBO revealed an approximate maximum temperature of 52°C for a lengthy 2 stack OLED run. The data from the run shown in Figure 35 was used in the conclusion. The peaks represent the max temperature as the substrate passed over a heated source. There are two groups because the run was stretched over two days. The largest peak at the end is from the silver deposition. To determine the worst case, the second group was shifted over and up 10°C to emulate a continuous run.

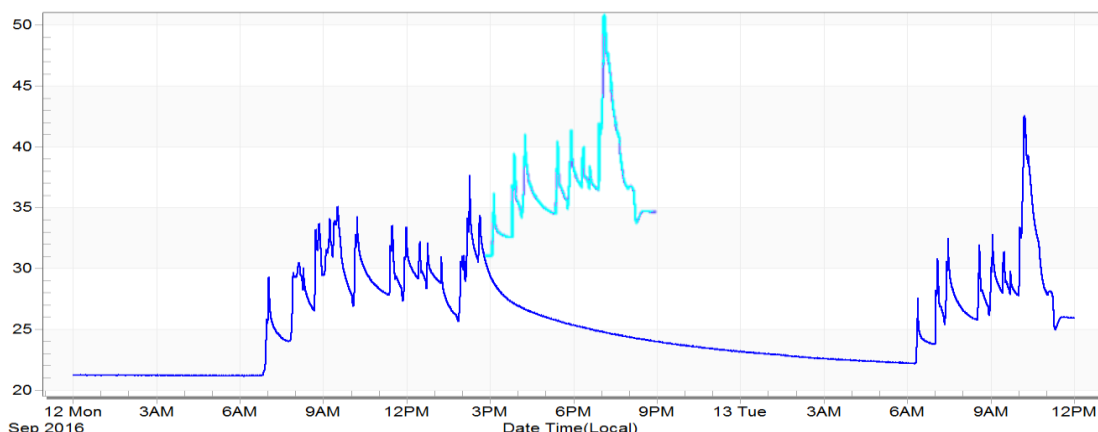


Figure 35. Substrate temperatures during complex run with worst case prediction.

OLED Device Performance After Cooling Improvements

OLED device performance is no longer degraded by the presence of the heated NGS. The experimental run data confirms radiometry and lifetime results are generally within spec and comparable to baseline controls. See Table 4 for a summary of the runs after the design improvements. Two materials, ET156 and HTM81, were deposited using the new source. One material per run was typically deposited using the NGS except for the 9/15 run where both materials were deposited.

Date	Experiment Description
160727	2U phos amber: Material A coated in two layers.
160728	2U phos amber: Material B coated in two layers.
160912	2U phos amber: Material A coated in two layers.
160913	2U phos amber: Material B coated in two layers.
160915	2U phos amber: Material A coated in two layers and Material B coated in two layers.
160919	2U phos amber: Control run: Original sources only. New Source is cool.
160920	2U phos amber: Material A coated in two layers.
160922	2U phos amber: Material B coated in two layers.

Table 4. Summary of runs after cooling improvements.

Initial OLED lifetime results were degraded compared to control runs. However, there is a strong trend, as shown by Figure 36, indicating the lifetime was improving with each run. Some minor residual contamination from the new components was likely the cause. Extrapolating the data suggested lifetimes would meet spec within a month.



Figure 36. Initial lifetime data after cooling improvements.

Figure 37 indicates the voltage variation and mean value of all the runs is comparable. The variation in the distribution is typical to prior control runs. The average voltage of 6.6V is slightly higher than the 6V specification.

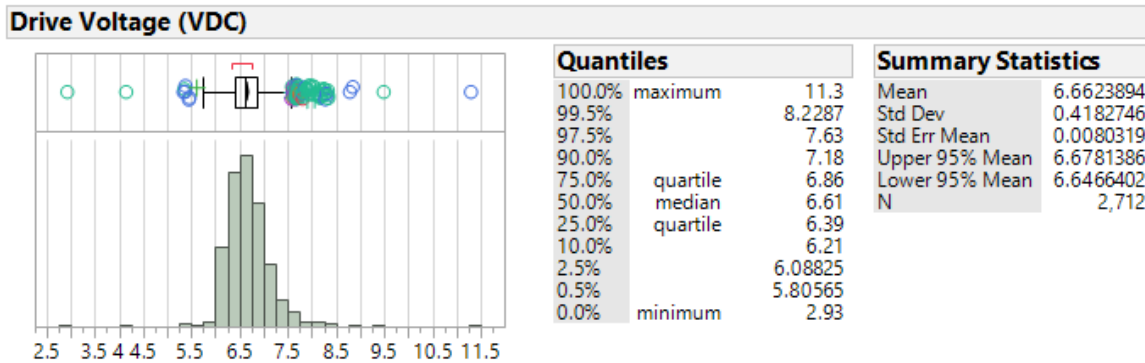


Figure 37. Voltage statistics for Table 4 runs.

Figure 38 shows most OLED devices are within the desired color bin (2). The NGS deposited OLED devices were closer to the desired color point than the control devices made only with the original sources.

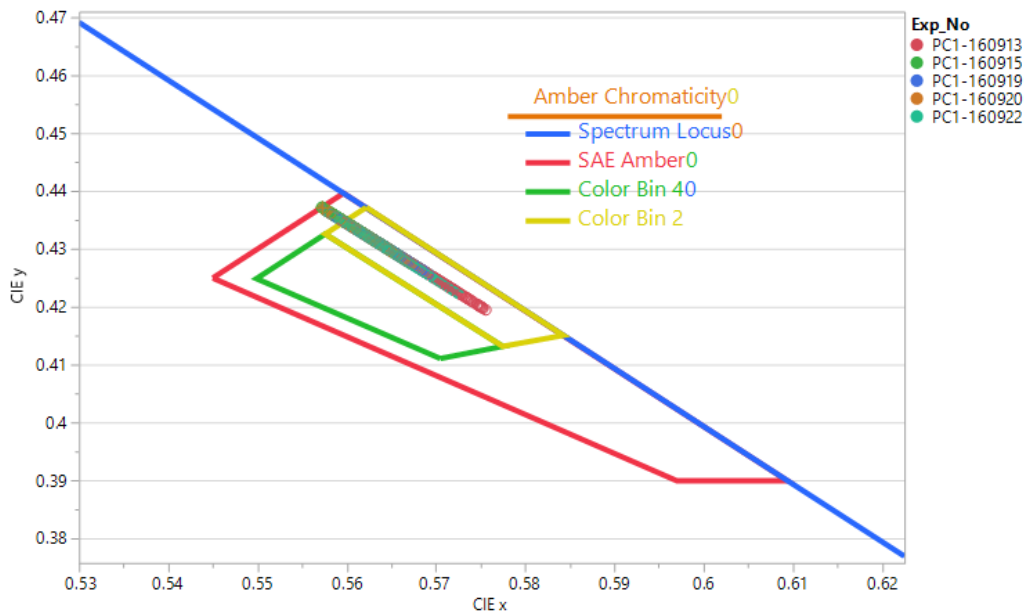


Figure 38. Color Comparison for Table 4 Runs. (NO EEL)

Additionally, the efficacies (lm/W) are comparable to the controls as displayed in Figure 39. The dotted line represents our baseline spec. All the efficacies appear low because no EEL was applied. EEL adds ~10 lm/W. In all experimental runs, Frame B devices had layers deposited using the NGS and Frame D devices, if present, were controls using only the original sources. The 9/19 run was a control with the NGS completely cooled. The NGS deposited devices from the 9/13, 9/15 (both materials deposited), and 9/20 (Quad D) runs are particularly good, even exceeding the controls.

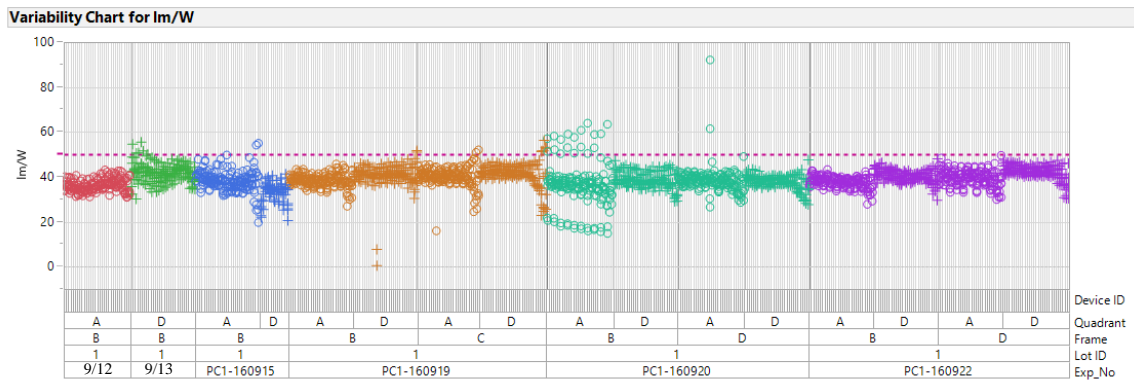


Figure 39. Efficacy comparison for Table 4 runs. (NO EEL: add ~10% efficacy).

Lifetime was also compared for four runs by measuring the relative light output over time at a higher current density. See Figure 40. To determine the predicted lifetime, the data is extrapolated to a relative light output of 70% and then corrected for the higher current density by using the following equation:

$$T_{norm} = T_{accl} \left(\frac{J_{accl}}{J_{norm}} \right)^{1.5} \text{ where } J = \text{current density}$$

The specification for lifetime is 25,000 Hrs. Lifetimes observed in the 9/15 run exceed the spec with a T_{70} of approximately 29,000 hours. These lifetimes are also greater than the lifetimes from the 9/19 control run. The 9/20 lifetimes are approximately the same as the control. The 9/22 run had variability issues due to complications during the run unrelated to the NGS.

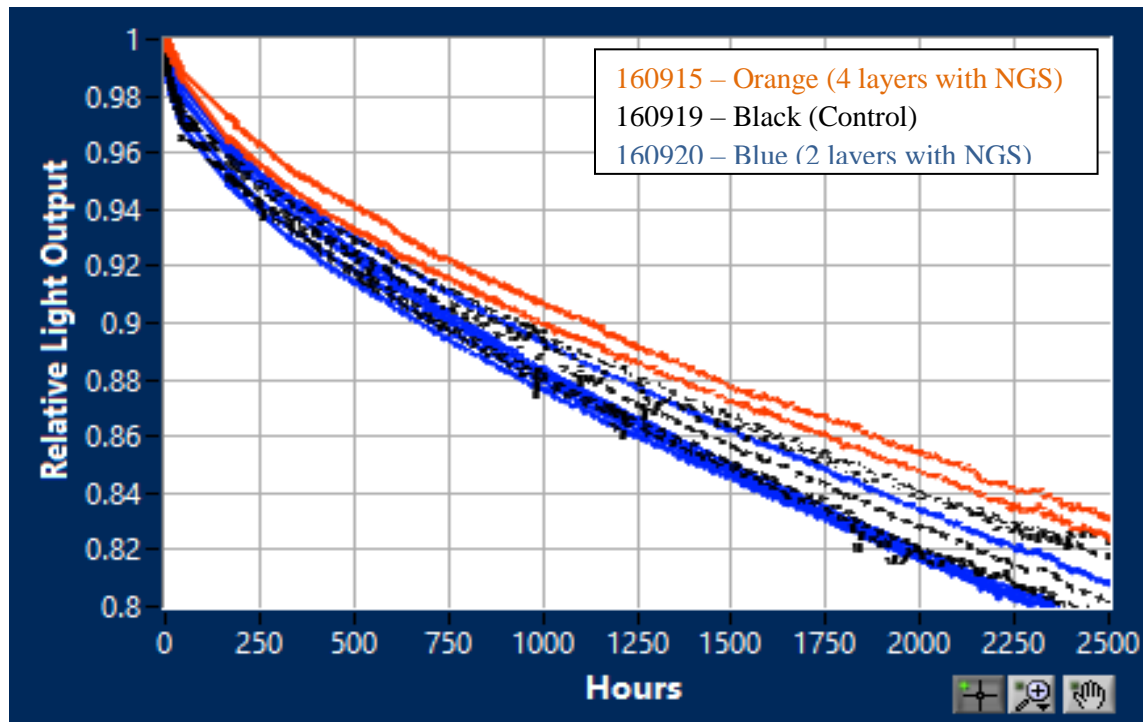


Figure 40. Accelerated device lifetimes for three runs (Marker Lights).

Design Improvement – Flexible Conduction Tube Connections

An important design improvement going forward was a flexible connection between the vaporizers and the conduction tubes. In the past, binding in the rate control valve, RCV, was observed due to the heating and expanding of the conduction tube. This expansion put unwanted stress on the RCV assembly and created misalignment in the RCV stem. Ultimately, the motor lacked the torque to turn the RCV. In the short term, this problem was fixed by increasing the tolerance in the coupling between the motor and valve stem.

With the addition of three more conduction tubes, expansion will occur in multiple dimensions. The expansion and contraction of each conduction tube would create complicated stresses on each other, the vaporizer assemblies, and connections. To absorb any displacement, flexible bellows-like connections, as shown in Figure 41, will link each CT and valve assembly. The bellows will replace the current conical reducer. The existing band heater on the 3.5" OD flange was replaced by a wider 3" band heater, also shown in Figure 41, to overlap and heat the bellows. The band heater is controlled to the desired temperature using built-in thermocouple.

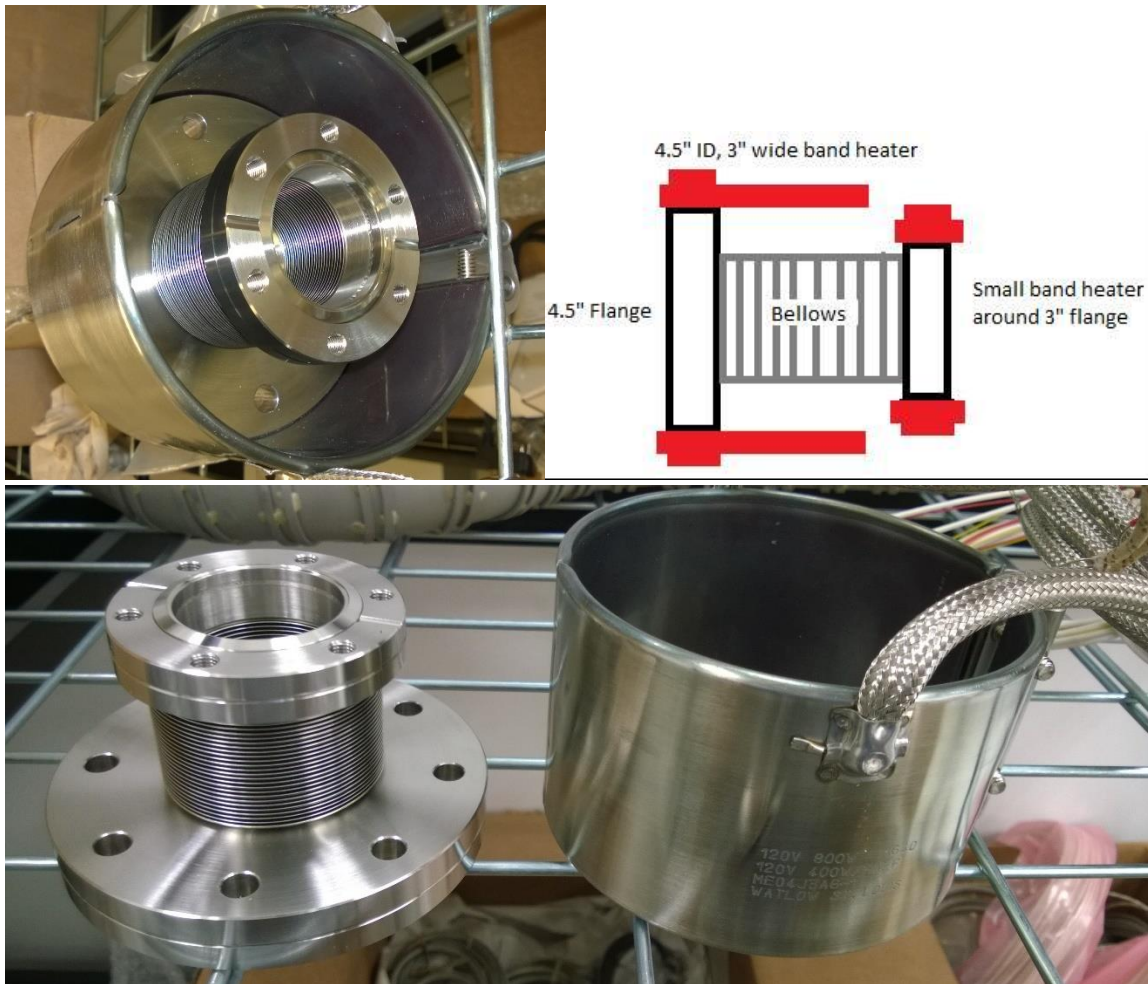


Figure 41. Flexible coupling w/ heater to link vaporizer and conduction tube.

Design Improvement – Material Crucible Alternative Design

The heated material crucible had trouble fully sealing which allowed material to condense between the heated crucible and ceramic holder. Figure 42 shows material re-condensed inside and behind the crucible. The sealing of the boat is essential to re-capturing and reusing vaporized material. These losses become negligible after saturating the spaces between the crucible and the ceramic holder. However, deformation during heating was still a concern.

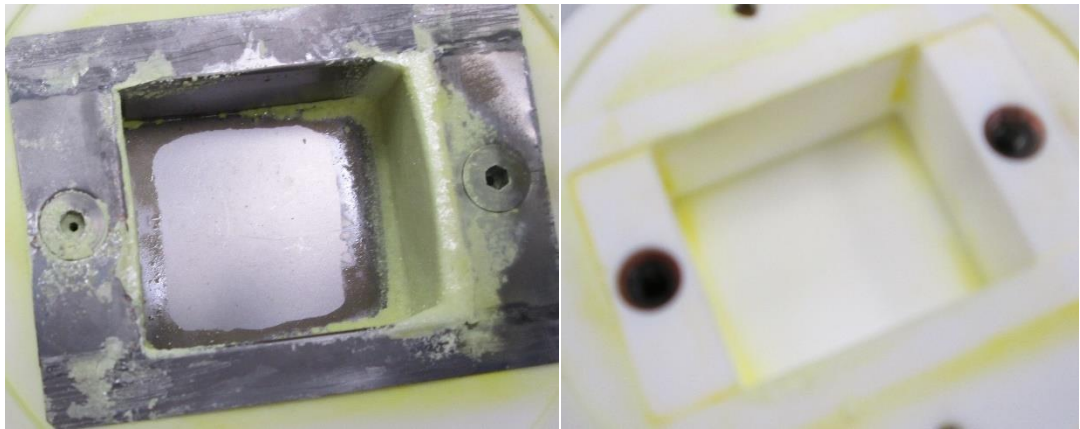


Figure 42. Material condensation on and behind heated crucible.

Therefore, a new heating element was designed where the heater floats within the ceramic holder. The ceramic holder becomes the material crucible in this design. The heating element heats the material by IR and conduction. See Figure 43. With this design, material cannot get trapped. There is a drawback with this design however. The heating of the element is greater than with the original design which results in greater thermal stresses on the ceramic crucible. Several crucibles were cracked while heating. A fix was implemented by gradually heating the materials.

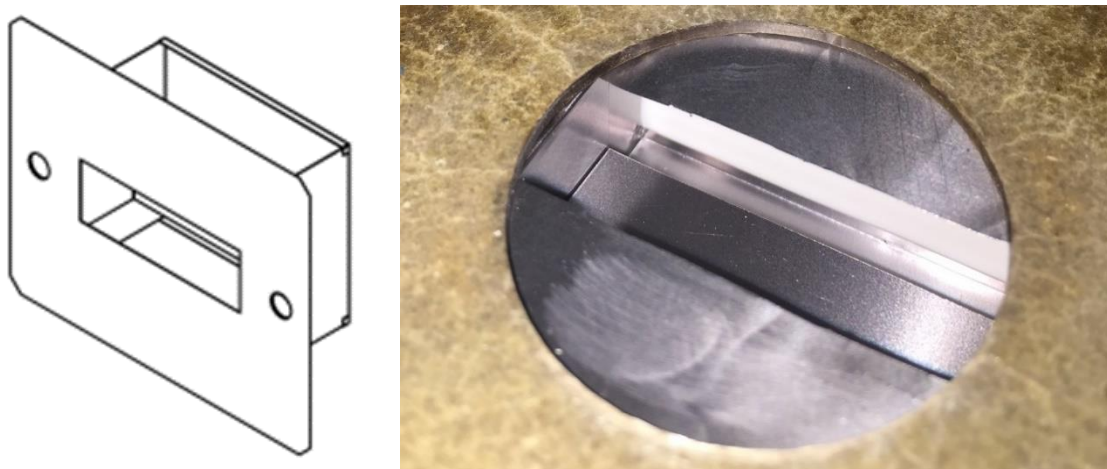


Figure 43. Floating heater design.

Both designs are still used based on the properties of the materials being used. The floating heater design is best for lower temp materials.

Design Improvement – Material Crucible Alternative Design

After the addition of the new source in the production coater, the base pressure of the chamber increased from 3E-7 torr to 1E-6 torr on average. The increase in pressure is due to the extra surface area added. The increase negatively affected device lifetimes. An additional cryo pump was purchased and installed to lower the base pressure of the chamber. See Figure 44. After the commissioning of the new cryo, the pressure returned to 3E-7 torr.

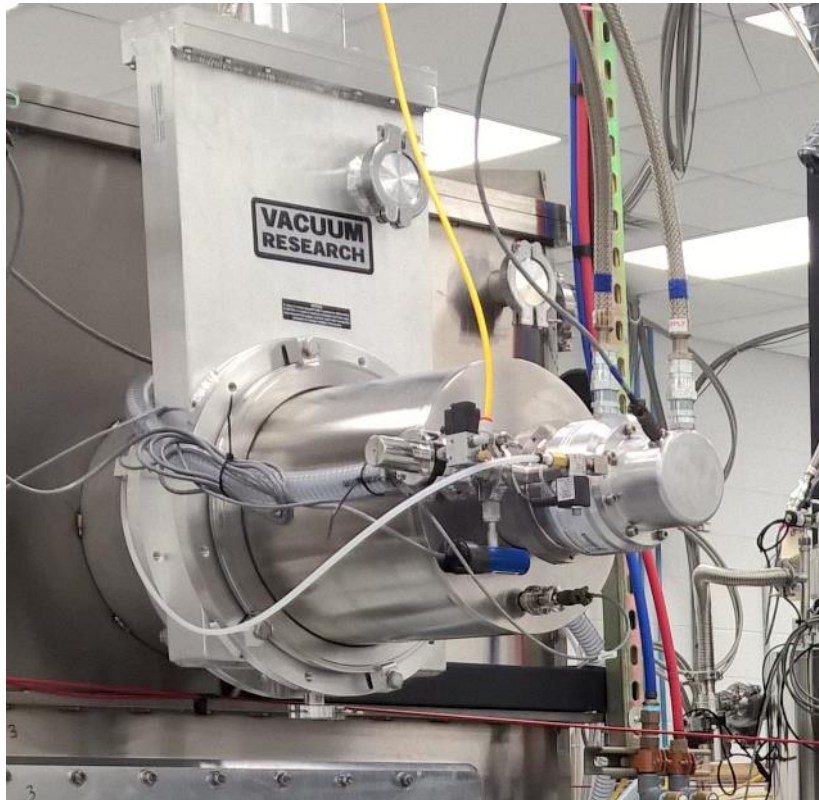


Figure 44. Cryo Pump Addition.

Task 5 – Build and Install Remaining Vaporizers and Nozzles

1. Four vaporizers and 4 nozzles were fabricated per the design in Task 4.
2. Design of integrated controls for all temperatures and vapor flow rates. Integrate into the system software of the production machine including – sensors, controls, interlocks, warnings, alarms, emergency conditions, data collection, and operator interface.
3. Modification of chamber to accept the new vaporizers and nozzles. Installation of utilities (electric supply, chilled water supply) required to support the new vaporizers and nozzles.
4. Installation of integrated set of 4 vaporizers and 4 nozzles into the production coater. This includes integration of the sensors, software, and controls for the new components into the existing software system.

In the prior section, the single vaporizer in combination with the newly water cooled four-component nozzle was thoroughly tested and debugged in the production coater. After successfully meeting the design criteria, three clones of the vaporizer were assembled and the next generation source was complete. See Figure 45. The prior design improvements were also implemented. All four vaporizers have independent material injection, rate control, and temperature control. Each corresponding conduction tube also has independent temperature control. The nozzle, however, is isothermal which limits all four component chambers to the same temperature. Therefore, the nozzle must match the temperature of the highest temperature material.

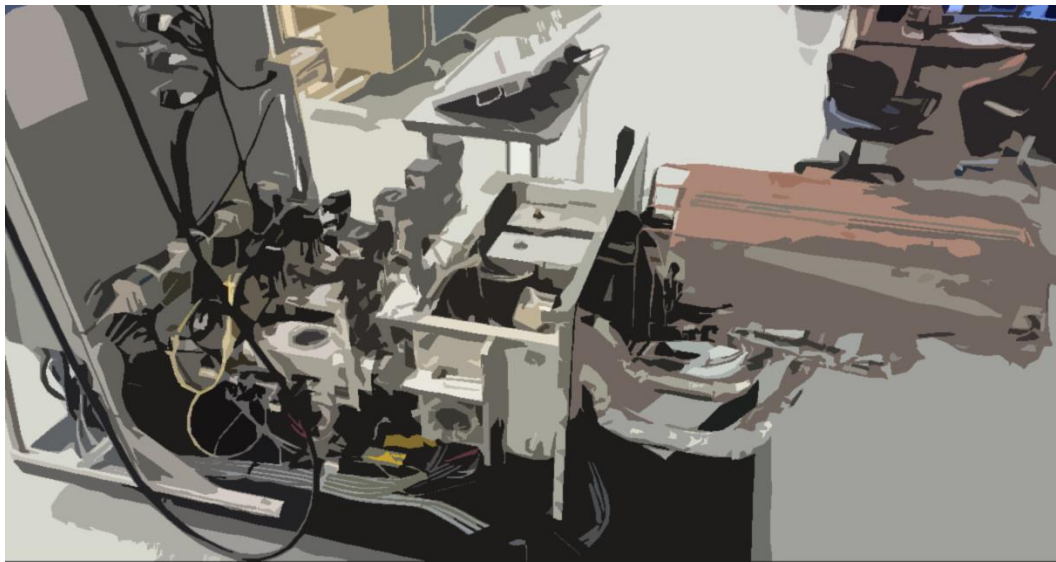


Figure 45. Next Generation Source – Complete System with Four Vaporizers.

The LabVIEW software was updated and integrated with the production equipment. The software, as depicted in Figure 46, provides operators with a graphical user interface for complete manual and automatic control over the new source. The software also reports faults and records real-time data for future analysis.

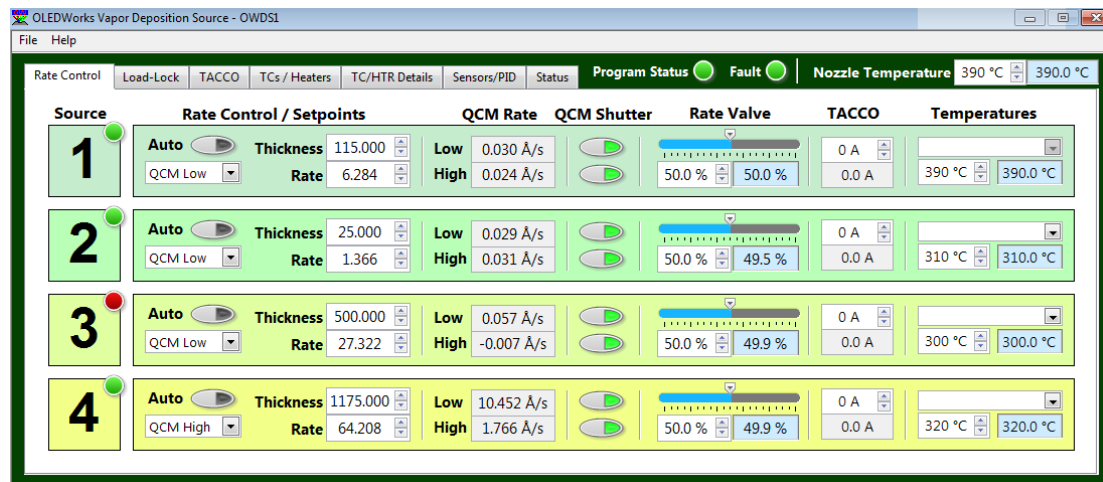


Figure 46. Software integration – GUI.

Task 6 – OLED Device Testing

The new sources were tested by making OLED devices side by side with the existing prototype sources. The performance of the new sources, as well as the limits of their capability, were determined for layers with 1, 2, 3, and 4 materials. The performance targets specific to the integrated set of 4 vaporizers and nozzles includes:

1. Testing of the integrated system against the physical performance targets for the system components from the previous tasks.
2. Cross talk between nozzles and rate sensors is low enough to allow good control of each nozzle independently.
3. Ability to deposit multi-component layers with and without heat sensitive materials with an average takt of 60 sec, with OLED performance comparable to devices made with the existing prototype sources.

All four vaporizers were tested and calibrated using the same procedures used with single vaporizer system. Each vaporizer was characterized, tuned and calibrated. The performance characteristics of the vaporizers are nearly identical. Afterwards, the co-deposition experiments were performed and OLED device performance was analyzed.

Figure 47 is included as an example of closed loop deposition control and calibration of vaporizer 3 of the new source. The rate as a function of power and valve position can be observed. The other vaporizers have similar control curves.



Figure 47. Screenshot of 3rd vaporizer deposition control.

Additional calibrations were run using the rates, materials, and temperatures typically used in a four-component deposition. The goal was to observe the actual thickness of each material deposited under normal operating circumstances compared to the predicted target thicknesses. The results of the measured thicknesses as a percentage of the target thicknesses are shown in Figure 48.

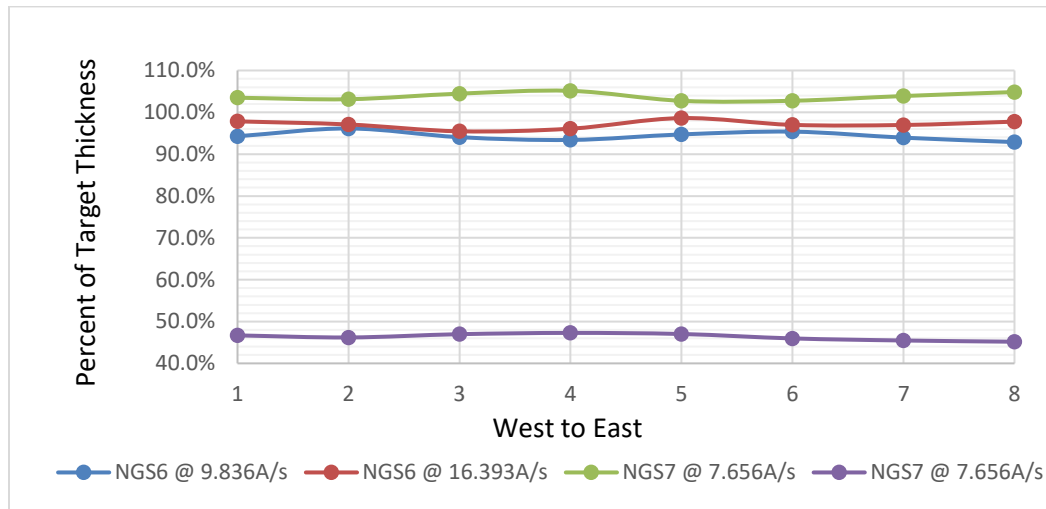


Figure 48. Calibrations of different materials and rates.

Evidently, all materials were deposited uniformly, $\pm 3\%$. Three of the four depositions met the expected thickness. The other was less than 50% of the expected thickness. The material used was a lower temperature material and degraded due to the high temperature of the nozzle. As mentioned previously, the nozzle temperature must be at least the temperature of the hottest vaporizer to prevent condensation of material in the nozzle. Consequently, the NGS is limited to co-depositions using materials with similar vaporization temperatures. Ideally the nozzle should be replaced with four thermally isolated chambers for optimal material flexibility. This improvement will not be covered within the scope of this project.

Therefore, several co-depositions experiments to deposit yellow emissive layers using the NGS were performed on March 1, 8, 13, 20, 22, and 28. Only materials with similar vaporization temperatures could be used. The yellow emissive layer is made from two co-deposited materials. Figure 49 depicts the co-deposition of two materials.

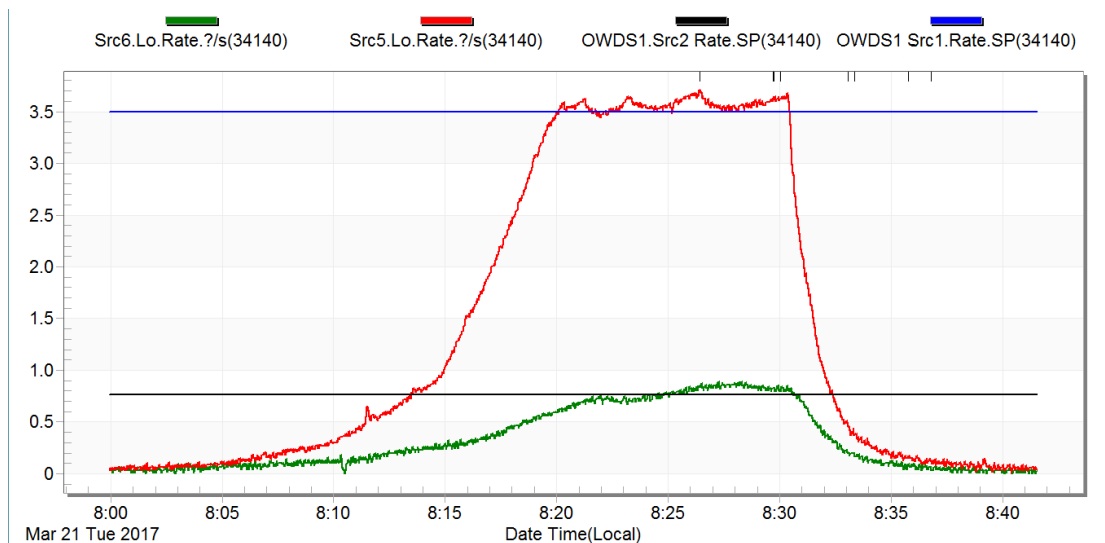


Figure 49. Two component deposition.

OLEDs produced using the NGS to co-deposit the yellow emissive layers have reduced lifetimes as shown in Figure 50. However, this is likely an initial affect as previously observed in the initial testing of the single vaporizer. New components have hard to clean contaminates that gradually come off while heated under vacuum. Fortunately, there is a consistent trend of improving lifetime with age as indicated by the arrow in Figure 50. Each run had improved lifetimes over prior runs, approaching the lifetimes of the control run (3/1/17).

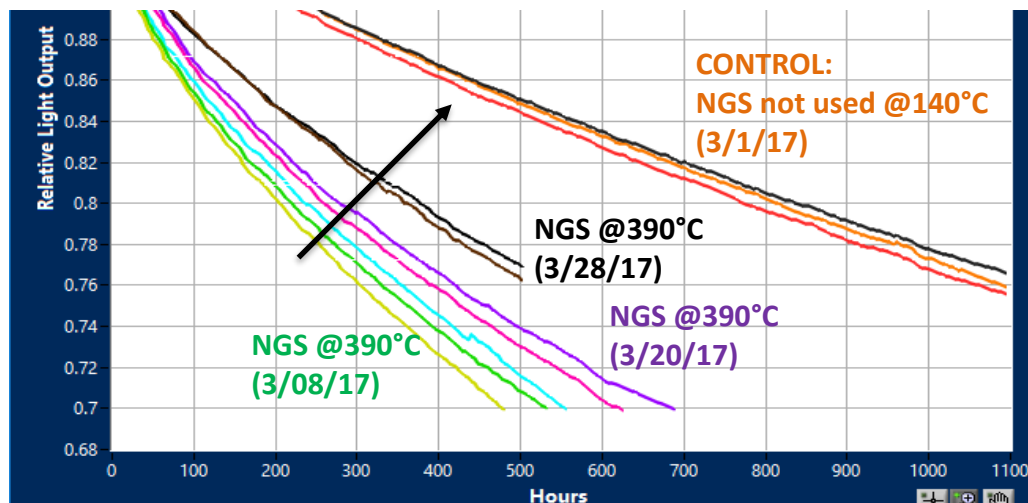


Figure 50. Lifetimes of OLED devices made after commissioning of competet NGS.

OLED devices produced had voltages close to the 6V spec. Variations in the earliest runs could be related to contaminates coming off the new vaporizers and conduction tubes. The last two runs had consistent voltages around 6.0 and 6.5V. See Figure 51.

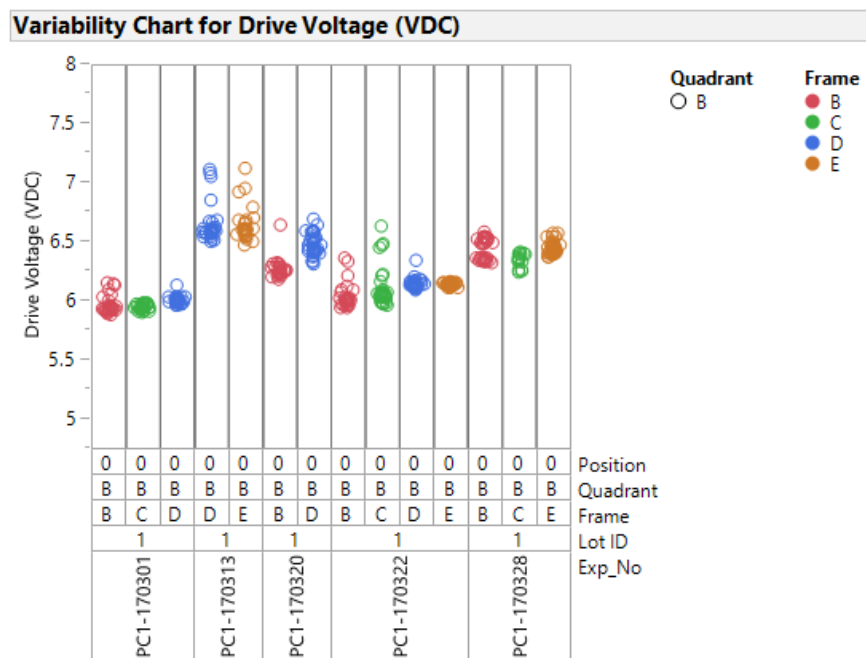


Figure 51. Voltages of OLED devices made after commissioning of competet NGS.

Run to run color was a moving target because of a faulty original source. Red dopant was intermittently leaked during most of the runs, changing the color point unpredictably. However, there was low in-run variation as shown in Figure 53. The last run of the project had all color points within OLEDWorks spec.

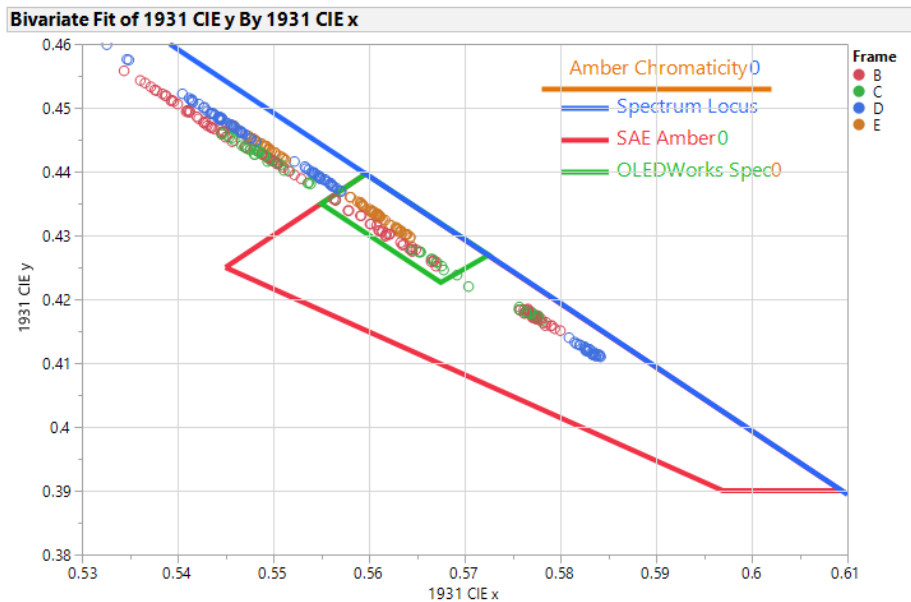


Figure 52. Color of OLED devices made after commissioning of competed NGS.

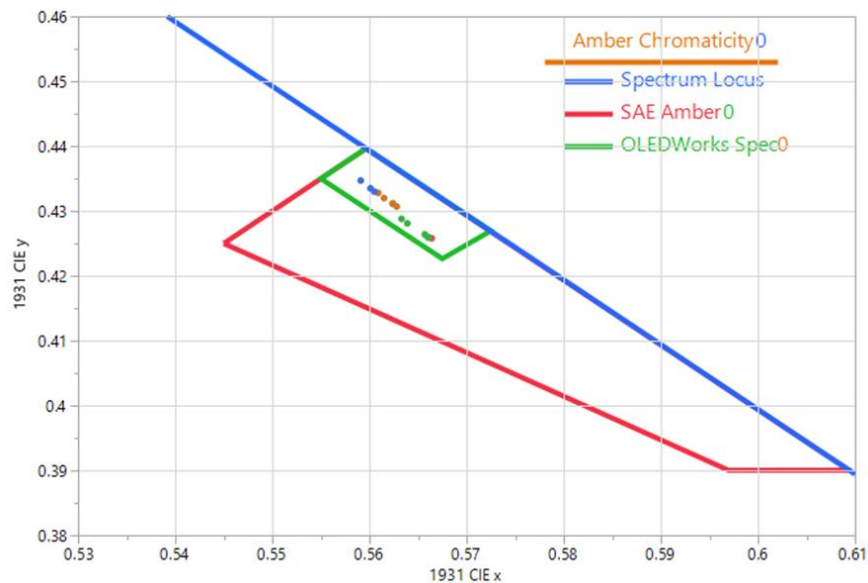


Figure 53. Color of OLED devices made on last run of project (3/28/17).

Lastly, OLED devices with the yellow emissive layer deposited by the NGS, two material co-deposition, had higher efficiencies than the control devices from the 3/1/17 run. See Figure 54. The variability observed is also due to the faulty original source leaking red dopant. The last run had low variability.

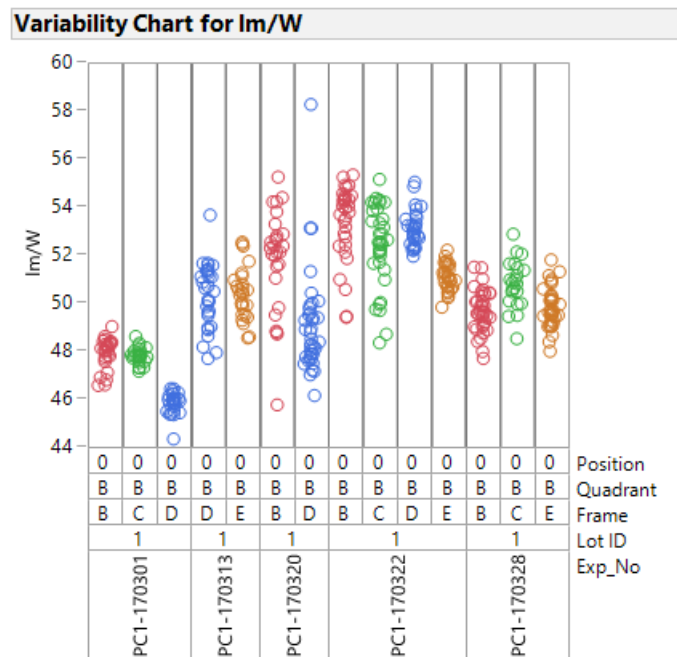


Figure 54. Efficiency of OLED devices made after commissioning of competited NGS.

Summary

The high-performance source works well when all the co-deposited materials have similar vaporization temperatures. Future improvements are planned to resolve any temperature limitations. Specifically, each chamber of the nozzle will be thermally isolated allowing independent temperature control. Other future improvements include a more robust material crucible and heated QCM collimating tubes to prevent material buildup and flaking.

Overall, the project was successful in meeting the proposed objectives. The new source has the potential to double production throughput while significantly reducing operational costs through material savings. This project has been invaluable in understanding, creating, and improving vacuum deposition technology for OLED development.

Project Output

The following product was developed under this award.

OLEDWorks produced a prototype high performance OLED deposition source capable of

- Four material co-depositions.
- Wide range rate deposition between 0.05Å/s and 60Å/s.
- Deposition uniformity of $\pm 3\%$.
- Material usage efficiencies up to 68%.
- Removing and inserting material.